JCB Journal of Cell Biology

ARTICLE

Range of SHH signaling in adrenal gland is limited by membrane contact to cells with primary cilia

Ivona Mateska[1,2], Kareena Nanda[3], Natalie A. Dye[1], Vasileia Ismini Alexaki[3], and Suzanne Eaton[1,2]

The signaling protein Sonic Hedgehog (SHH) is crucial for the development and function of many vertebrate tissues. It remains largely unclear, however, what defines the range and specificity of pathway activation. The adrenal gland represents a useful model to address this question, where the SHH pathway is activated in a very specific subset of cells lying near the SHH-producing cells, even though there is an abundance of lipoproteins that would allow SHH to travel and signal long-range. We determine that, whereas adrenal cells can secrete SHH on lipoproteins, this form of SHH is inactive due to the presence of cosecreted inhibitors, potentially explaining the absence of long-range signaling. Instead, we find that SHH-producing cells signal at short range via membrane-bound SHH, only to receiving cells with primary cilia. Finally, our data from NCI-H295R adrenocortical carcinoma cells suggest that adrenocortical tumors may evade these regulatory control mechanisms by acquiring the ability to activate SHH target genes in response to TGF-β.

Introduction

The Hedgehog (Hh) signaling cascade determines the fate and growth of many animal tissues during development, adult homeostasis, and disease (Ingham and McMahon, 2001). Hh is a secreted protein that can travel long distances (up to 300 µm) through tissues to affect gene expression in a concentration-dependent manner during development (Briscoe and Thérond, 2013). Multiple mechanisms have been shown to facilitate long-range transport of the hydrophobic Hh ligand, including secretion on lipoproteins (Panáková et al., 2005; Palm et al., 2013) and exovesicles (Vyas et al., 2014). Nonetheless, in many adult vertebrate organs, where Hh is required for homeostatic maintenance, pathway activity is more restricted (Petrova and Joyner, 2014). The mechanisms defining where, when, and to what extent the Hh pathway becomes activated in these vertebrate tissues are largely unknown.

Sonic Hedgehog (SHH) is the most ubiquitous mammalian Hh homologue (Ingham et al., 2011). Once it travels to receiving cells, SHH signals by repressing the activity of its receptor, Patched1 (PTCH1), a transmembrane protein with a sterol-sensing domain (Kuwabara and Labouesse, 2002). PTCH1 regulates the accessibility of small lipidic molecules that activate or inhibit another transmembrane protein, Smoothened (SMO; Taipale et al., 2002; Khaliullina et al., 2009). Once activated, SMO relocates to the tip of the primary cilium (Corbit et al., 2005; Rohatgi et al., 2007; Milenkovic et al., 2009), a signaling organelle found in many mammalian cells (Christensen et al., 2007). In the primary cilium, SMO activates a signaling cascade that changes the posttranslational processing of glioma-associated oncogene (GLI) family transcription factors, promotes formation of their activator forms, and ultimately leads to transcription of Hh target genes (Haycraft et al., 2005; Tukachinsky et al., 2010; Humke et al., 2010; Hui and Angers, 2011).

Determining how SHH is produced and received is critical for understanding what limits the range of its activity. Lipoproteins are required for the release and long-range transport of the SHH ligand and its signaling output (Eaton, 2008). Additionally, lipoproteins carry Hh pathway inhibitors, such as endocannabinoids (Khaliullina et al., 2009, 2015). Only sufficient amounts of lipid-modified SHH loaded in parallel on lipoproteins can overcome this inhibition (Palm et al., 2013). Alternatively, Hh can be secreted on exovesicles (Tanaka et al., 2005; Vyas et al., 2014) or can signal via direct cell-to-cell contacts (Rojas-Ríos et al., 2012; Bischoff et al., 2013; Sanders et al., 2013; Gradilla et al., 2014). Signaling by direct cell contact would presumably limit Hh signaling to short range, although there are examples of long cell protrusions carrying Hh in *Drosophila melanogaster* (Kornberg and Roy, 2014).

[1]Max Planck Institute of Molecular Cell Biology and Genetics, Dresden, Germany; [2]Biotechnologisches Zentrum, Technische Universität Dresden, Dresden, Germany; [3]Institute of Clinical Chemistry and Laboratory Medicine, Technische Universität Dresden, Dresden, Germany.

Dr. Eaton died on July 2, 2019; Correspondence to Ivona Mateska: mateska@mpi-cbg.de; I. Mateska's present address is Institute of Clinical Chemistry and Laboratory Medicine, Technische Universität Dresden, Dresden, Germany.

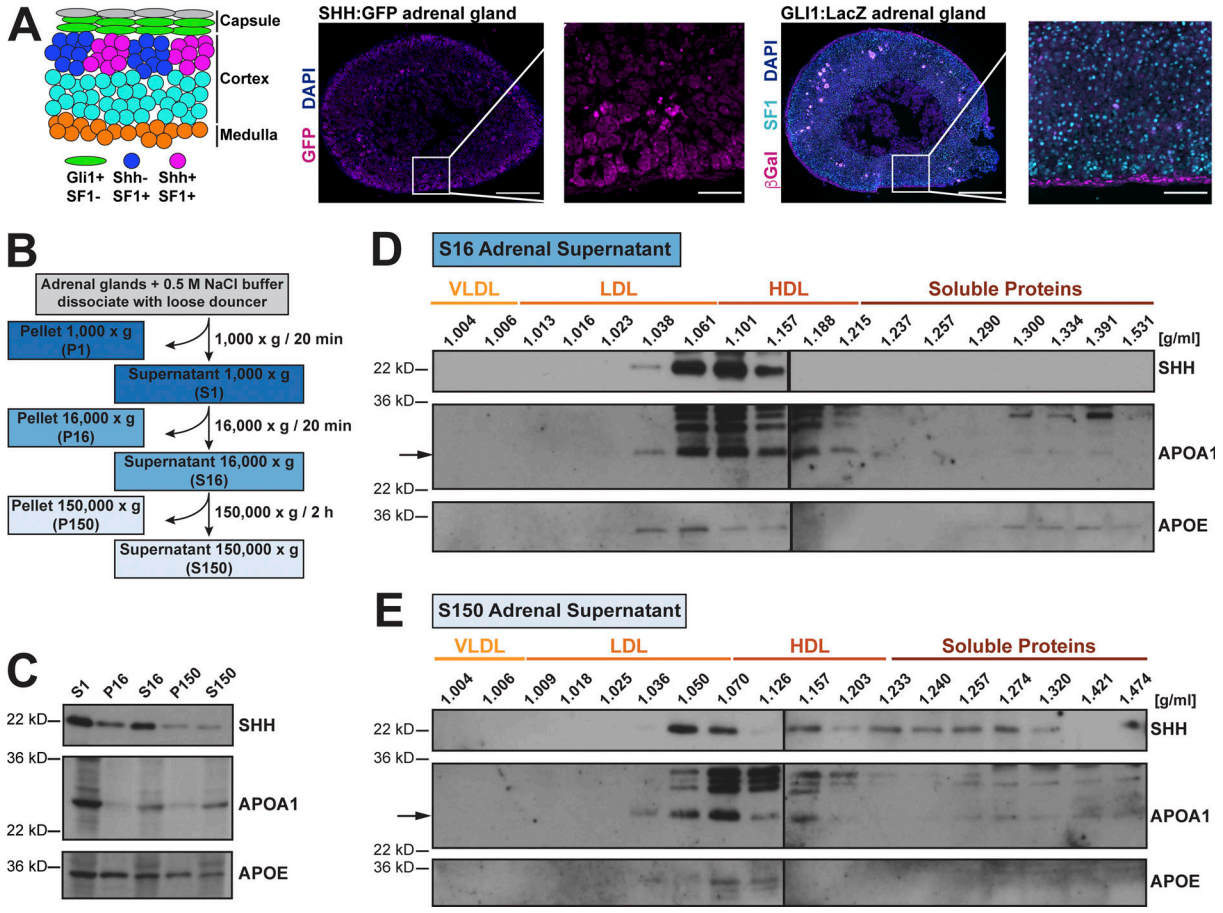

Figure 1. **SHH produced by mouse adrenal glands cofractionates with lipoproteins. (A)** Left: Schematic representation of the zones and cell types in the mouse adrenal gland. SHH is produced by subset of subcapsular cortical cells, positive for the steroidogenic marker SF1 (magenta). Right: Adrenal gland sections from Shh^{GFP} mice stained for GFP and DAPI and $Gli1^{LacZ}$ mice stained for β-galactosidase and SF1. For each staining, a magnification is shown. Scale bar, 300 µm. **(B)** Experimental scheme for the isolation and differential centrifugation of SHH from mouse adrenal glands. **(C)** Western blots of adrenal fractions separated by differential centrifugation, probed for SHH or lipoprotein markers (APOA1, APOE). **(D and E)** Western blot of density gradient fractions from adrenal supernatants at 16,000 *g* (D) and 150,000 *g* (E), blotted for SHH and lipoprotein markers (APOA1, APOE). Density of lipoprotein classes is according to Jonas and Phillips (2008). The experiment was repeated three times with similar results. VLDL, very-low-density lipoproteins.

The adrenal gland represents an interesting model to address the question of how short- versus long-range SHH signaling is regulated. The adrenal gland is an endocrine organ with essential functions in mammals that requires SHH for its development and adult homeostasis (Yates et al., 2013). It has an ample access to lipoproteins, as they are the major source of cholesterol for steroid hormones biosynthesis (Kraemer, 2007). Yet it is still unknown whether endogenously produced SHH can be secreted on lipoproteins, as it is in some cell lines (Palm et al., 2013), or whether it can signal in an alternative form. Although there is an abundance of lipoproteins, which would allow SHH to travel and signal long-range, SHH pathway activation is limited to short-range interactions between two adrenal compartments: the adrenal cortex consisting of steroidogenic (SF1-positive) cells and the overlaying mesenchymal capsule (Fig. 1 A; Keegan and Hammer, 2002). Clusters of undifferentiated steroidogenic cells of the outer adrenal cortex produce SHH, which signals specifically to the adjacent nonsteroidogenic capsule cells (Ching and Vilain 2009; King et al., 2009; Guasti et al., 2011). These cells respond by expressing the SHH target genes, *Gli1* and *Ptch1*, and producing terminally differentiated lineages (King et al., 2009; Huang et al., 2010; Laufer et al., 2012; Freedman et al., 2013). Other cells of the cortex do not activate the SHH pathway—neither those in close proximity to the producing cells nor those far away (Wood and Hammer, 2011). How specific, short-range SHH signaling occurs even in the presence of lipoproteins is an important open question.

Importantly, ectopic overactivation of the SHH pathway in the adrenal gland has been implicated in disease, such as obesity and adrenal carcinoma. In both cases, no increase in the amount of the SHH ligand itself is seen (Gomes et al., 2014; Swierczynska et al., 2015; Werminghaus et al., 2014), making it unclear how the pathway is up-regulated. In the case of obesity, overactivated SHH pathway in capsule progenitors (SHH-receiving cells) results in an expanded cortex and elevated levels of steroid hormones in mice (Swierczynska et al., 2015). In the case of adrenocortical tumors, SHH pathway components and target genes are overexpressed (Boulkroun et al., 2011; Gomes et al., 2014), and antagonizing the pathway reduces growth of the NCI-H295R adrenocortical carcinoma cell line (Werminghaus et al.,

2014). How the pathway may be involved in adrenal cancer is unclear, however, as examples for both autocrine and paracrine SHH signaling promoting tumor growth can be found in other cancer types (Berman et al., 2003; Watkins et al., 2003; Yauch et al., 2008; Chan et al., 2012). Furthermore, it is unknown whether the SHH ligand itself is required, as a crosstalk between the SHH and TGF-β pathways exists in many tumors (Dennler et al., 2007; Javelaud et al., 2011).

Here, we address the mechanisms limiting the range and specificity of SHH signaling in normal and cancerous adrenocortical cells. We find that SHH can be released on lipoproteins, but this pool is signaling inactive, possibly due to lipoprotein-associated pathway inhibitor(s). Instead, SHH signaling occurs via membrane contact, limiting the signaling range. We suggest that the specificity of SHH signaling is limited by the presence of primary cilia in receiving cells. Adrenocortical cells that produce SHH, both in vivo and in a carcinoma cell line, lack ARL13B-positive primary cilia and are unable to respond to the SHH ligand they produce. Importantly, the carcinoma cell line evades the requirement for SHH ligand by ectopically expressing SHH pathway target genes in response to TGF-β. These findings provide novel, fundamental, and potentially clinically relevant insight into mechanisms regulating SHH pathway signaling range and activity.

Results

Mouse adrenal glands secrete SHH on lipoproteins

To address how the specific range of SHH signaling is achieved in the adrenal gland, we first determined whether adrenocortical cells can secrete SHH associated with lipoproteins. To do so, we compared the distribution of SHH in a density gradient to that of apolipoprotein (APO) A1 and APOE, the major protein components of high-density lipoproteins (HDL; Hegele, 2009). We fractionated high-salt adrenal gland homogenates by differential centrifugation at 16,000 *g* and 150,000 *g* (Fig. 1, B and C) and subjected both supernatant fractions to isopycnic density centrifugation (Fig. 1, D and E; Palm et al., 2013). The majority of SHH in 16,000 *g* supernatants was found in lower-density fractions. Its distribution in the density gradient resembled that of APOA1 and, to a lesser extent, APOE (Fig. 1 D). The 150,000 *g* supernatants were additionally enriched in a higher-density pool of SHH (Fig. 1 E). We conclude that the adrenal glands can secrete SHH in fractions containing lipoproteins.

Given the importance of diet in regulating SHH pathway activity in the adrenal gland (Swierczynska et al., 2015), we investigated whether lipoproteins affect SHH secretion in the adrenal gland in mice with diet-induced obesity. We observed, however, no change in the fractionation of SHH or in the level or density of lipoproteins in the adrenals from mice fed with normal and high-fat diets (HFDs; Fig. S1 A). Furthermore, the density of released SHH in adrenal supernatants was also not affected (Fig. S1, B and C). Thus, the elevated SHH signaling in the adrenals of mice fed a HFD does not appear to be caused by increased release of SHH or any obvious alterations in the released forms.

In culture, human adrenocortical carcinoma cells endogenously secrete SHH on lipoproteins

As an alternative model for probing SHH secretion and signaling in adrenal gland cells, we engaged the human adrenocortical carcinoma cell line NCI-H295R. These cells have been extensively used to study adrenal function and tumor biology (Gazdar et al., 1990; Rainey et al., 2004) and express *SHH* mRNA (Werminghaus et al., 2014). To confirm that this cell line accurately represents the SHH release mechanisms of adrenal glands, we asked whether and how NCI-H295R cells secrete SHH protein. Western blot analyses verified that NCI-H295R cells endogenously produce SHH (Fig. 2, A and B). Sera from different species (bovine, murine, and human) can act as a source of lipoproteins to enhance SHH release into the culture medium, but do not contain SHH (Fig. 2, B and C). Despite producing and secreting lipoproteins, NCI-H295R cells require extrinsically added serum supplement for SHH secretion (Fig. 2 D). Upon fractionating conditioned medium from NCI-H295R cells, we found that serum supports the release of a low-density SHH pool that is intermediate between low-density lipoproteins (LDLs) and HDL, cofractionating with APOA1 and APOE lipoproteins (Fig. 2, E–G). We also observed an additional higher-density pool of SHH in the supernatant of cells incubated with human serum (Fig. 2 G). The forms of SHH released from these cells closely resemble those isolated from the mouse adrenal gland in vivo (compare to Fig. 1, D and E), providing confidence that this cell line is an appropriate model for studying SHH release from adrenocortical cells.

To confirm that lipoproteins are sufficient for SHH release, we cultured NCI-H295R cells only with lipoproteins isolated from human serum and assayed the conditioned medium by density gradient centrifugation. We found that addition of human lipoproteins promotes the release of SHH in a low-density form, consistent with LDL and HDL densities, but no SHH fractionates at higher densities (Fig. 3, A–C). Western blotting of gradient fractions with antibodies to apolipoproteins (APOA1 and APOE) showed that these proteins are present in the same low-density fractions as SHH (Fig. 3 C). Thus, SHH secreted from NCI-H295R cells can associate with lipoproteins. To confirm this, we precipitated cell supernatants with antibodies to apolipoproteins and found that SHH immunoprecipitates with APOA1 and, less efficiently, APOE (Fig. 3 D). Based on the cofractionation of SHH with LDL and HDL and its coimmunoprecipitation with APOA1 and APOE, as well as previous reports (Palm et al., 2013), we conclude that adrenocortical carcinoma cells can release endogenously produced SHH on lipoproteins.

The lipoprotein-associated SHH secreted from adrenocortical carcinoma cells is signaling-inactive

The above data indicate that both adrenal glands and adrenocortical carcinoma cells produce and secrete SHH on lipoproteins, which should facilitate long-range transport. Given the limited long-range signaling in the adrenal gland, we sought to determine whether this form of secreted SHH is actually signaling-active. Thus, we next analyzed the canonical (Gli1-dependent) signaling activity of lipoprotein-associated SHH using the Shh-LIGHT2 reporter expressed in NIH3T3 fibroblasts

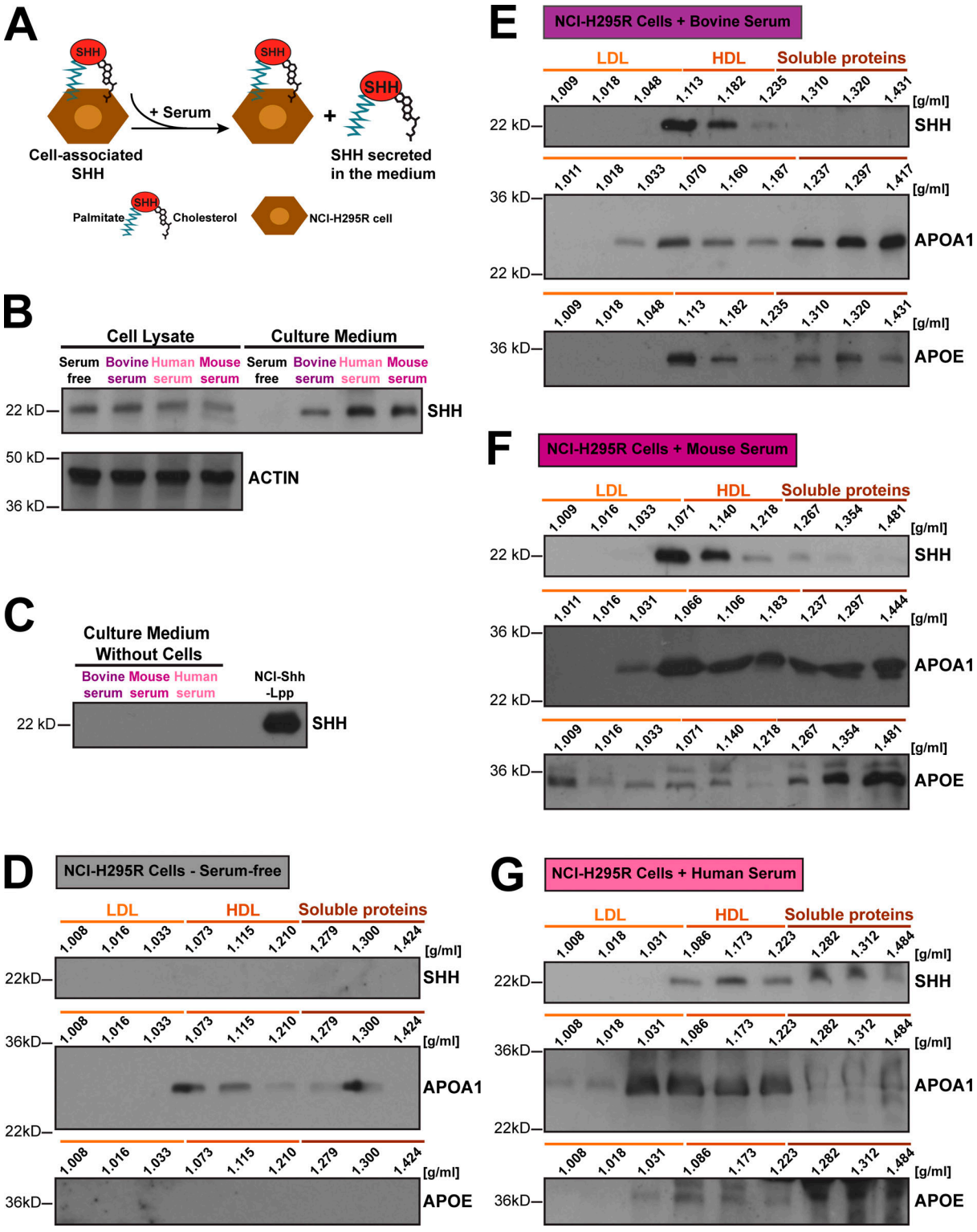

Figure 2. **Adrenocortical carcinoma cells cultured with serum supplement endogenously produce and secrete SHH, which cofractionates with LDL and HDL. (A)** NCI-H295R cells produce and secrete SHH into the culture medium in the presence of serum supplement. **(B)** Western blot of cell lysates and conditioned medium from NCI-H295R cells, cultured in serum-free conditions or with bovine, mouse, or human serum, probed for SHH. Equal amounts of cell lysates and corresponding conditioned medium were loaded. ACTIN was used as a loading control for the cell lysates. **(C)** Western blot of culture medium supplemented with different sera, probed for SHH. Conditioned medium from NCI-H295R cells cultured with human lipoproteins (NCI-Shh-Lpp) was loaded as reference. **(D–G)** Western blots of density gradient fractions of conditioned medium from NCI-H295R cells cultured in serum-free medium (D) or with bovine (E), mouse (F), or human (G) serum, probed for SHH, APOA1, or APOE. Density of lipoprotein classes is according to Jonas and Phillips (2008).

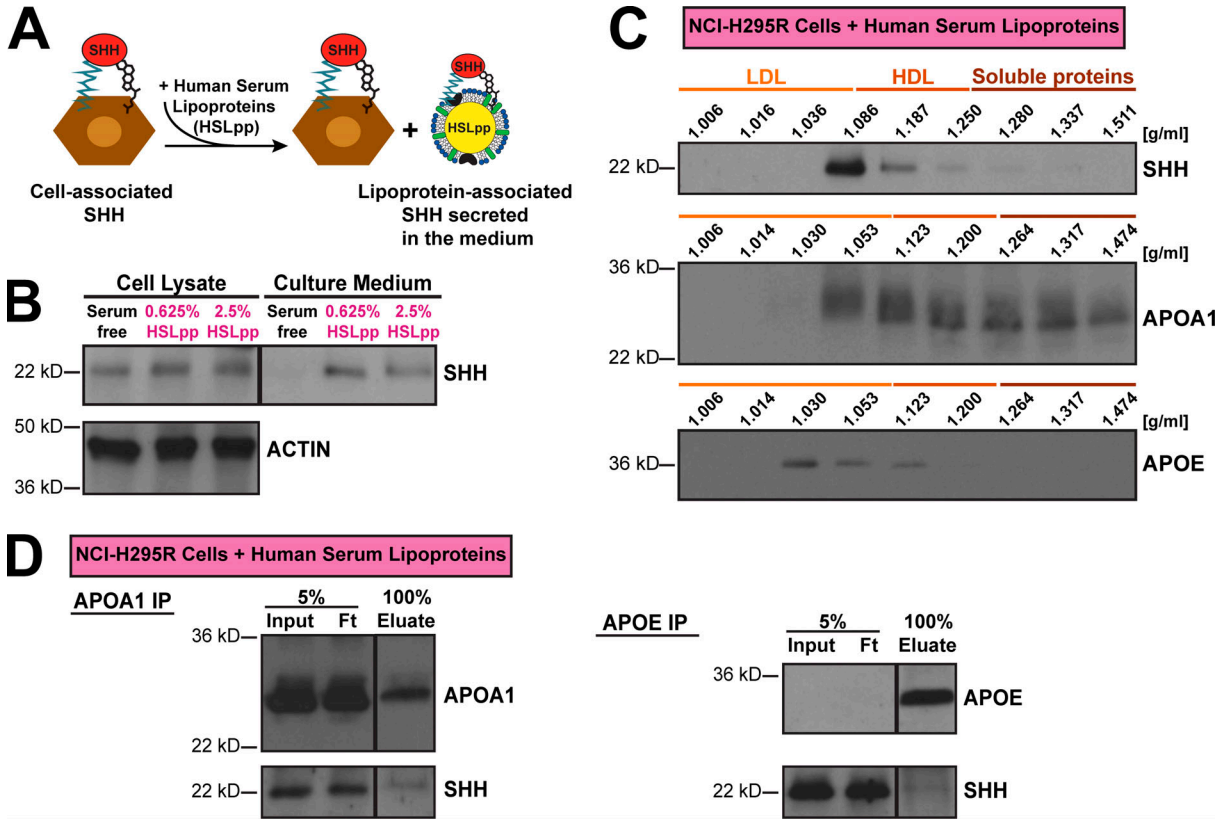

Figure 3. **Lipoproteins are necessary and sufficient for secretion of lipoprotein-associated SHH from adrenocortical carcinoma cells in vitro.** **(A)** Secreted SHH from NCI-H295R cells associates with lipoproteins. **(B)** Western blot of cell lysates and conditioned medium from NCI-H295R cells cultured in serum-free conditions or with 0.625% or 2.5% human serum lipoproteins (HSLpp), probed for SHH. Equal amounts of cell lysate and corresponding conditioned medium were loaded. ACTIN was used as a loading control for the cell lysates. **(C)** Western blots of density gradient fractions of conditioned medium from NCI-H295R cells cultured with human serum lipoproteins, probed for SHH, APOA1, or APOE. The density of lipoprotein classes is according to Jonas and Phillips (2008). **(D)** Western blots of immunoprecipitation with antibodies to apolipoproteins APOA1 and APOE from conditioned medium of NCI-H295R cells grown with human serum lipoproteins, probed for the corresponding immunoprecipitated (IP) protein and SHH. Ft, flow-through.

(Fig. 4 A; Taipale et al., 2000). Compared with human embryonic kidney (HEK)-293 cells stably transfected with SHH and HeLa cells transiently engineered to produce SHH, NCI-H295R cells endogenously secrete low concentrations of SHH on lipoproteins (Fig. S2 A). At this low concentration, none of the SHH preparations signal in the Shh-LIGHT2 assay, compared with the SMO agonist SAG, which strongly induces the LIGHT2 signal (Fig. 4 B and Fig. S2 B). Therefore, we concentrated the NCI-H295R-derived conditioned medium and assayed its SHH signaling activity. At higher concentrations, lipoprotein-associated ShhNc (cholesterol-modified SHH) derived from HEK-293 and HeLa cells induces a potent signaling response; however, lipoprotein-associated SHH derived from NCI-H295R is still inactive (Fig. 4 C).

We wondered whether the reason for the inactive SHH was that NCI-H295R cells also secrete inhibitor(s) of the pathway, as was shown in other contexts (Khaliullina et al., 2015). To test this possibility, we added conditioned media from NCI-H295R cells to active concentrations of lipoprotein-associated ShhNc from HEK-293 cells. Indeed, we found that the NCI-H295R–conditioned media cause a dose-dependent inhibition of the signaling activity of HEK-derived ShhNc (Fig. 4 D and Fig. S2 C). This result is not due to an impact of the NCI-H295R–conditioned medium on the viability or ciliation of the Shh-LIGHT2 cells (data not shown). Moreover, conditioned medium from HeLa cells does not inhibit the SHH pathway (Fig. S2 D), indicating that the inhibition does not originate from the serum or the media themselves but is specific to media conditioned by NCI-H295R cells. While it is possible that NCI-H295R cells produce a signaling-inactive SHH isoform that can compete with HEK-derived ShhNc for its receptor PTCH1, the lowest amount of NCI-H295R–produced SHH that is inhibitory is 100× less than that of the added HEK-derived ShhNc (Fig. 4 D). Thus, it is highly unlikely that the inhibition is due to inhibition at the level of the ligand/receptor interaction but rather downstream. Confirming this hypothesis, we found that NCI-H295R–conditioned medium inhibits the activation of SMO by the SMO agonist SAG, which activates the pathway independently of the ligand (Fig. 4 E). To determine whether normal adrenocortical tissue also secretes this inhibitory molecule(s), we tested homogenates of mouse adrenal glands, as well as conditioned media from primary mouse adrenal cell cultures. Both cause a dose-dependent inhibition of the signaling activity of HEK-ShhNc (Fig. 4, F and G). The lowest volume of adrenal cell culture supernatant required for SHH pathway inhibition (1 µl; Fig. 4 G) corresponds to the secretome of ∼500 adrenal cultured

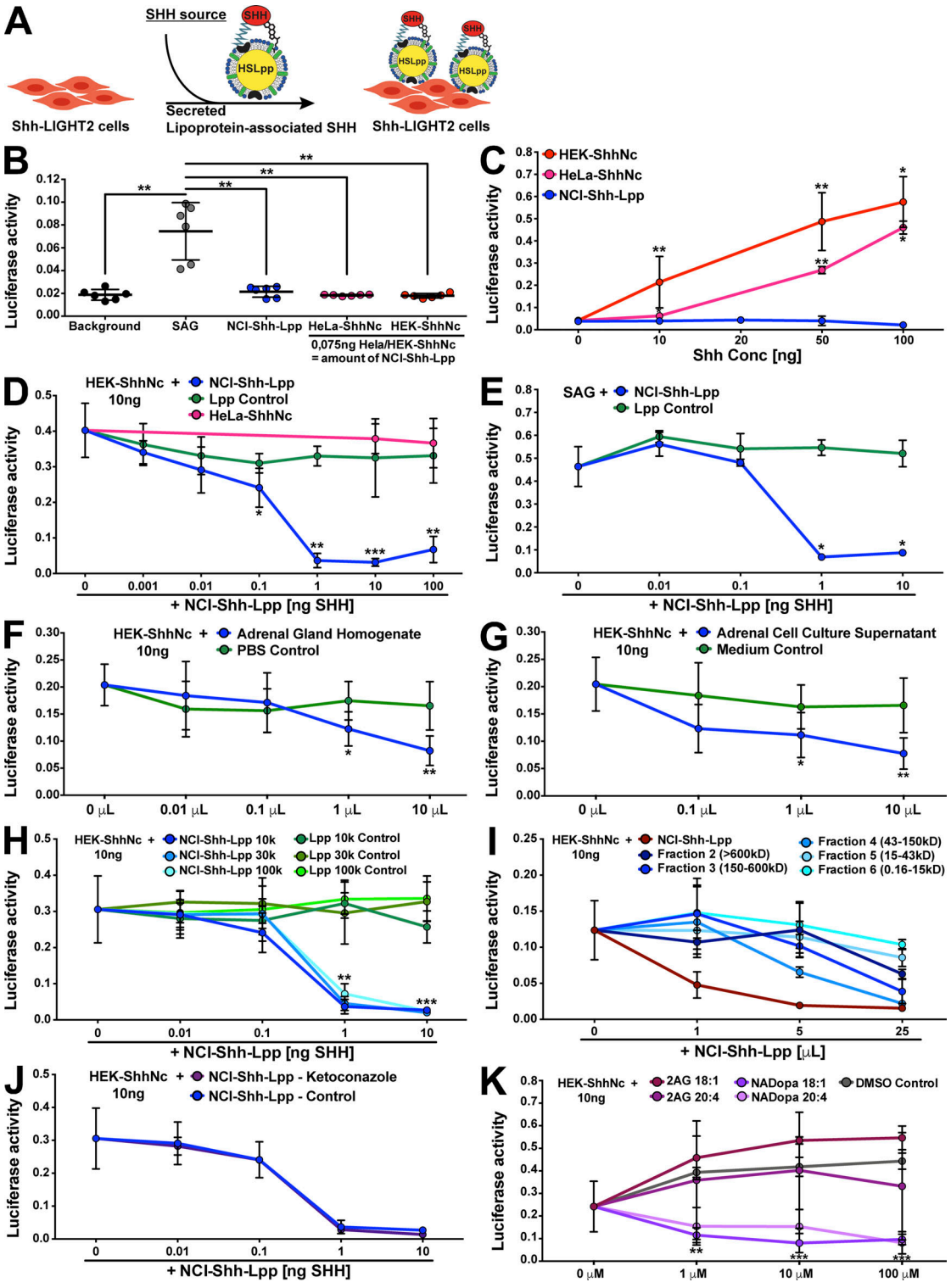

Figure 4. **Lipoprotein-associated SHH secreted from adrenocortical carcinoma cells is signaling-inactive, due to an inhibitory molecule(s) also secreted from these cells. (A)** Schematic representation of the experiment. Shh-LIGHT2 mouse fibroblasts were treated with conditioned medium containing secreted, lipoprotein-associated SHH. **(B)** Shh-LIGHT2 cells were treated with unconcentrated NCI-H295R–conditioned medium or with the corresponding amounts of conditioned medium from SHH-transfected HEK-293 and HeLa cells (HEK-ShhNc and HeLa-ShhNc, respectively). Treatment with the SMO agonist SAG is a positive control for the Shh-LIGHT2 assay activity. **(C)** Shh-LIGHT2 cells were treated with increasing amounts of concentrated conditioned medium from SHH-transfected HEK-293 and HeLa cells (HEK-ShhNc and HeLa-ShhNc, respectively), and from NCI-H295R cells (NCI-Shh-Lpp). **(D and E)** Shh-LIGHT2 cells were treated with (D) 10 ng HEK-ShhNc or (E) 200 nM SAG, together with increasing amounts of NCI-H295R–conditioned medium. **(F–K)** Shh-LIGHT2 cells were treated with 10 ng HEK-ShhNc together with increasing amounts of (F) adrenal gland homogenate or PBS lysis buffer control; (G) conditioned medium from primary adrenal gland cell cultures or medium control; (H) NCI-H295R–conditioned medium or Lpp control medium cleared through 10-, 30-, and 100-kD size filters; (I) whole NCI-H295R–conditioned medium (NCI-Shh-Lpp) or size fractions separated by gel filtration chromatography; (J) conditioned

medium from NCI-H295R cells treated with 10 µM ketoconazole or vehicle control; (K) endocannabinoid lipids or vehicle control. The Lpp Control represents medium with added human serum lipoproteins, not cultured with NCI-H295R cells. Data are presented as mean ± SD, *n* = 4–6 replicates, pooled from two or three experiments. *, P < 0.05; **, P < 0.01; ***, P < 0.001. 2AG, 2-acylglycerol; NADopa, N-acyldopamine.

cells. In contrast, the lowest volume of NCI-H295R supernatant showing SHH pathway inhibitory activity (Fig. 4, D, E, and H) corresponds to the secretome of ∼55,000 NCI-H295R cells, implying that the primary adrenal cell culture supernatant has at least 100× more potent inhibitory effect than the NCI-H295R supernatant. Hence, our results indicate that although adrenocortical cells can secrete SHH on lipoproteins, this signaling form is inactive, due to an inhibitory molecule(s) that is cosecreted and blocks the SHH pathway at the level or downstream of SMO.

Next, we set out to characterize this inhibitor(s). We found that the inhibitory activity of the NCI-H295R supernatant is retained by filters up to a 100-kD cutoff (Fig. 4 H), and gel filtration chromatography identified inhibitory activity in fractions corresponding to estimated molecular weights of 43–600 kD (Fig. 4 I). These results suggest that the inhibitory activity is contained in large complexes that, consistent with their size, may be lipoproteins (German et al., 2006; Frazier-Wood et al., 2011). Considering the fact that the adrenal gland is the major producer of steroid hormones, we examined whether blocking steroidogenesis with ketoconazole (Nielsen et al., 2012) could affect the inhibitory activity of NCI-H295R supernatants. We found, however, that inhibiting steroidogenesis in NCI-H295R cells does not affect the inhibitory activity of the conditioned medium (Fig. 4 J). As alternative candidates, we considered endocannabinoids: anandamide, 2-arachidonoylglycerol, and endocannabinoid homologues containing various fatty acyl chain lengths including N-acyldopamines, which were shown to be lipoprotein-associated and repress the Hh/SHH pathway in *Drosophila* and mammalian cells (Khaliullina et al., 2015). Out of 18 tested endocannabinoid lipids, we found that N-acyldopamine 18:1 and 20:4 inhibit HEK-ShhNc activity, while others, such as 2-acylglycerol 18:1 and 20:4, were not inhibitory (Fig. 4 K). These results, together with the reported abundance of dopamine and arachidonic acid (C 20:4) in mouse adrenal glands (Igal et al., 1991; Campbell et al., 1991), suggest that N-acyldopamine 20:4 can act as an inhibitor of SHH signaling in the adrenal gland.

Membrane-associated SHH on adrenocortical carcinoma cells signals to adjacent fibroblasts

Since the secreted SHH pool from NCI-H295R cells appears to be unable to signal, we wondered whether these cells may be able to signal in a different way. In other systems, the Hh ligand can also signal by direct contact through membrane extensions (Kornberg and Roy, 2014). The existence of such a mechanism seems plausible in the adrenal gland, where SHH-producing cortical cells lie in close proximity to the SHH-responding capsular fibroblasts (Fig. 1 A; Guasti et al., 2011; Laufer et al., 2012).

Upon co-culturing Shh-LIGHT2 fibroblasts with NCI-H295R cells (Fig. 5 A), we found potent induction of Gli1-dependent reporter activity in the fibroblasts (Fig. 5 B). The increase in Gli1-dependent transcriptional activity is completely abolished by treatment with the SHH-neutralizing antibody 5E1 and the pathway antagonist cyclopamine, verifying that it is specifically mediated by activation of the SHH pathway (Fig. 5 B). Two lines of evidence suggest that signaling occurs via the membrane-associated SHH. First, the addition of lipoproteins should induce lipoprotein-mediated SHH secretion from NCI-H295R cells, thereby decreasing the pool of membrane-associated SHH. Indeed, SHH pathway activity in Shh-LIGHT2 cells is higher under serum-free conditions, when SHH is mostly cell-associated, than in the presence of lipoproteins (Fig. 5, B and C). Second, Gli1-dependent transcription in Shh-LIGHT2 cells is induced only upon co-culture with NCI-H295R cells in direct physical contact and not when sharing the culture medium (Fig. 5 C). As an alternative readout of SHH pathway activity, we visualized SMO localization in responding NIH3T3 cells transfected with Smo-mEos2, a reporter of SMO localization. We co-cultured NIH3T3/Smo-mEos2 cells with increasing numbers of NCI-H295R cells in serum-free media, with the prediction that more NCI-H295R cells would increase the number of cell–cell contacts and thereby cause increased SMO ciliary localization. Indeed, we observe a concentration-dependent enrichment of SMO in primary cilia (Fig. 5, D and E). Importantly, the ciliation rate of fibroblasts is not affected by the co-culture with carcinoma cells (data not shown). Thus, the membrane-associated SHH, rather than the lipoprotein-associated secreted SHH, is responsible for the SHH signaling activity of adrenocortical carcinoma cells, suggesting a contact-dependent activation of the SHH pathway in the responding fibroblasts.

Adrenocortical carcinoma cells do not respond to SHH ligand

The inhibitory activity within the lipoprotein fraction of secreted SHH, combined with the signaling-active membrane-bound SHH, partially explains the limited range of SHH signaling in the adrenal gland. However, it remains unclear why the SHH pathway is activated only in the overlaying capsule cells but not in the adrenocortical cells located in close proximity to the SHH-producing cells. Normal murine adrenal cortex and NCI-H295R cells express the key pathway transducers PTCH1 and SMO (Fig. 6, A–C), indicating that they could respond to the SHH they produce. However, normal adrenal cortex cells do not express the SHH targets GLI1–3 (Fig. 6, A and C), while NCI-H295R cells, which derive from adrenocortical carcinoma, do express these genes (Fig. 6, B and C), indicating that they may have acquired the ability to respond to the SHH they produce, as do many other tumors (Wetmore, 2003).

We investigated whether the carcinoma cell line had acquired the ability to respond to SHH, in order to determine whether pathway activation is differently regulated in these two contexts. We found, however, that repressing or activating SHH signaling does not affect the proliferation of NCI-H295R cells (Fig. 6 D). Furthermore, expression of the SHH target genes *GLI1* and *PTCH1* in NCI-H295R cells is unaffected by treatment with

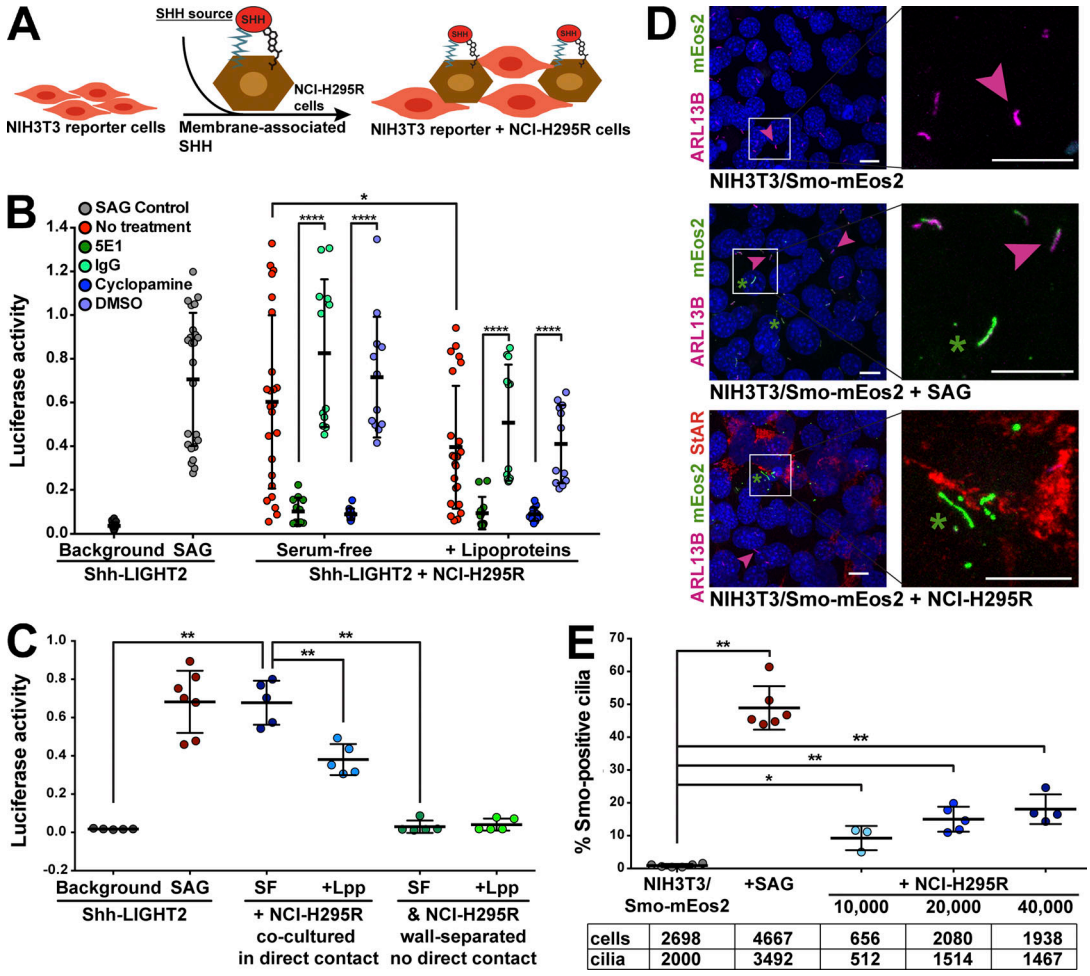

Figure 5. **Membrane-associated SHH on adrenocortical carcinoma cells signals to adjacent fibroblasts. (A)** Schematic representation of the experiment. Mouse fibroblasts were co-cultured adjacent to NCI-H295R cells. In B and C, Shh-LIGHT2 were used for measuring luciferase activity as a readout of *Gli1* transcription, while in D and E, NIH3T3/Smo-mEos2 were used for direct visualization of SMO enriched in primary cilia. **(B)** Shh-LIGHT2 cells were co-cultured in direct contact with NCI-H295R, in the presence or absence of lipoproteins, and treated with 10 µg/ml 5E1, 10 µM cyclopamine, or the appropriate controls. Data are presented as mean ± SD, *n* = 12–24 replicates, pooled from 3–6 experiments. *, P < 0.05; ****, P < 0.0001. **(C)** Shh-LIGHT2 and NCI-H295R cells were co-cultured either in direct contact or in wall-separated culture inserts, where they share the same culture medium. SAG treatment was used as a positive control for Shh-LIGHT2 activity. Data are presented as mean ± SD, *n* = 5–7 replicates, pooled from three experiments. **, P < 0.01. **(D)** Immunofluorescence of 40,000 NIH3T3/Smo-mEos2 cells, treated either with 200 nM SAG or co-cultured with 40,000 NCI-H295R cells, labeled for ARL13B–cilia (magenta), Smo-mEos2 (green), StAR, a steroidogenic marker present in mitochondria of NCI-H295R cells (red), and nuclear DAPI (blue). ARL13B-positive cilia are denoted with magenta arrowheads. Ciliary SMO enrichment is indicated with an asterisk. Scale bar, 10 µm. **(E)** Quantification of the percentage of NIH3T3/Smo-mEos2 cells with ciliary SMO enrichment. The number of cells and cilia counted is given under each experimental condition. Data are presented as mean ± SD, *n* = 4–6 replicates, pooled from two experiments. *, P < 0.05; **, P < 0.01.

the SHH-blocking antibody 5E1, the SMO antagonist cyclopamine (Fig. 6 E), the pathway agonist SAG, or ShhNc derived from HEK-293 cells (Fig. 6 F). In contrast, NIH3T3 cells robustly activate *Gli1* and *Ptch1* expression in response to SAG and ShhNc from HEK-293 cells, in a 5E1-dependent manner (Fig. 6 G). Thus, we conclude that the active membrane-associated SHH produced by adrenocortical carcinoma cells cannot activate the canonical SHH pathway in an autocrine manner. We also considered the possibility that adrenocortical carcinoma cells respond noncanonically to SHH (Teperino et al., 2014). SHH was shown to reprogram cell metabolism toward the Warburg-like state (Teperino et al., 2012) and to reduce intracellular cAMP levels (Riobo et al., 2006; Shen et al., 2013). However, we do not observe similar effects of SHH pathway activation in NCI-H295R cells (Fig. S3, A–D).

We conclude that adrenocortical carcinoma NCI-H295R cells do not respond to the SHH they produce, nor to SHH from other sources, either in canonical or noncanonical ways. Furthermore, the inability of the SMO agonist SAG to activate the pathway in adrenocortical carcinoma cells suggests that these cells not only do not bind the ligand but also cannot respond to activated SMO.

Adrenocortical cells in vitro and in vivo lack ARL13B-positive primary cilia

Neither healthy nor cancerous adrenocortical cells appear to be able to respond to the SHH they produce, highlighting a key part of how the specific pattern of signaling activity is achieved in the adrenal gland. To investigate the underlying mechanism, we considered the critical role of primary cilia in SHH pathway

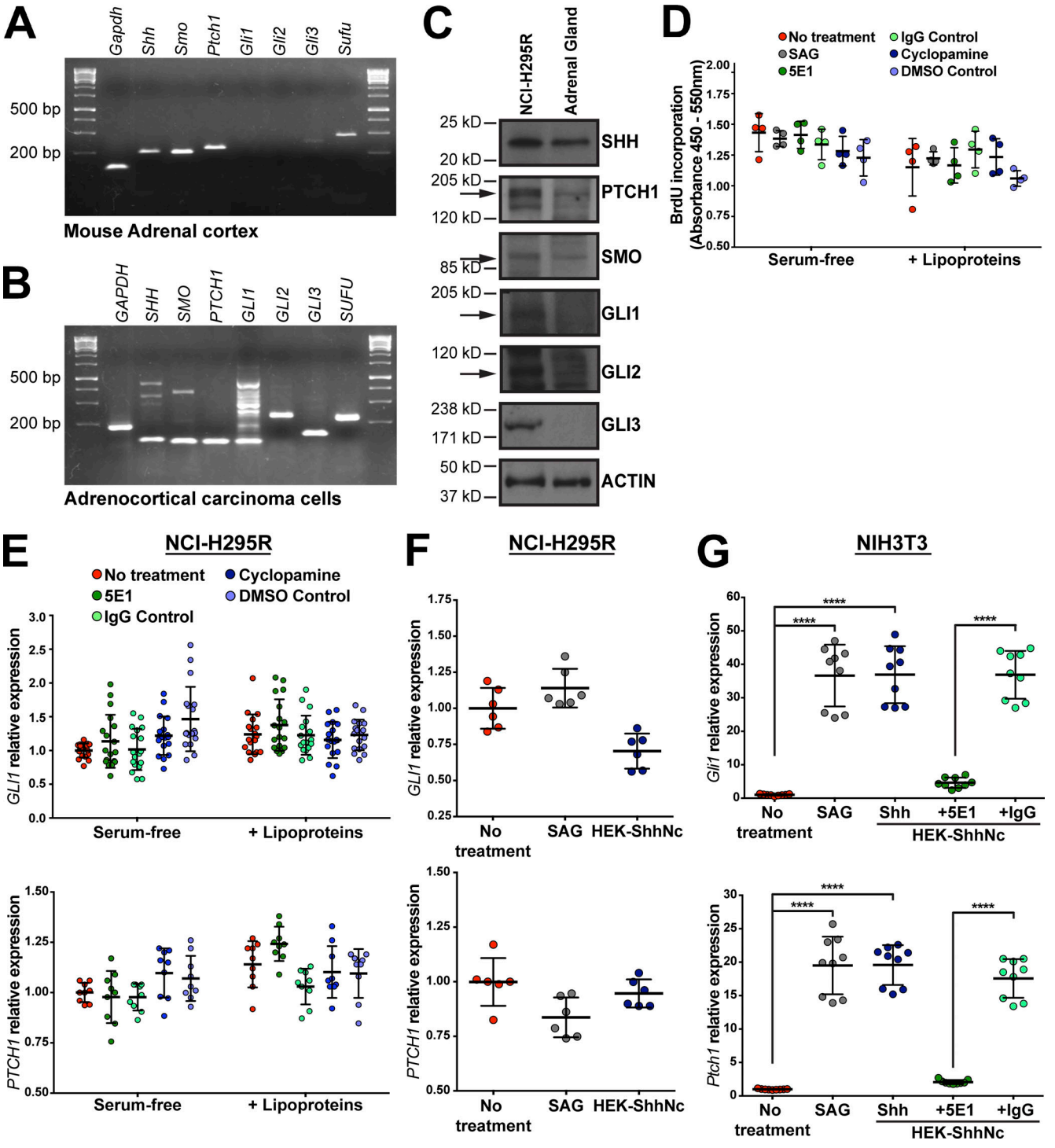

Figure 6. **Human adrenocortical carcinoma cells do not exhibit autocrine, canonical SHH signaling. (A)** Semiquantitative RT-PCR showing the expression of SHH pathway components in mouse microdissected adrenal cortex, using *Gapdh* as a reference. **(B)** Semiquantitative RT-PCR showing the expression of SHH pathway components in NCI-H295R cells, using *GAPDH* as a reference. **(C)** Western blots of NCI-H295R cell and adrenal gland lysates, probed for SHH, PTCH1, SMO, GLI1, GLI2, GLI3, and ACTIN as a loading control. **(D)** Proliferation of NCI-H295R cells cultured with or without lipoproteins with the respective treatments, quantified by measuring BrdU incorporation. Data are presented as mean ± SD, $n = 4$ replicates, pooled from two experiments. **(E and F)** *GLI1* and *PTCH1* expression in NCI-H295R cells grown for 48 h with or without lipoproteins, treated with SHH pathway inhibitors 10 µg/ml 5E1 and 10 µM cyclopamine or appropriate controls (E), or with SHH pathway activators 200 nM SAG or 10 ng HEK-ShhNc (F). **(G)** *Gli1* and *Ptch1* expression in mouse fibroblasts NIH3T3 is used as a positive control for canonical SHH signaling. *B-actin* is used as a reference. Data are normalized to the respective No treatment values. **(E–G)** Data are presented as mean ± SD, $n = 6–12$ replicates, pooled from two to four experiments. ****, $P < 0.001$.

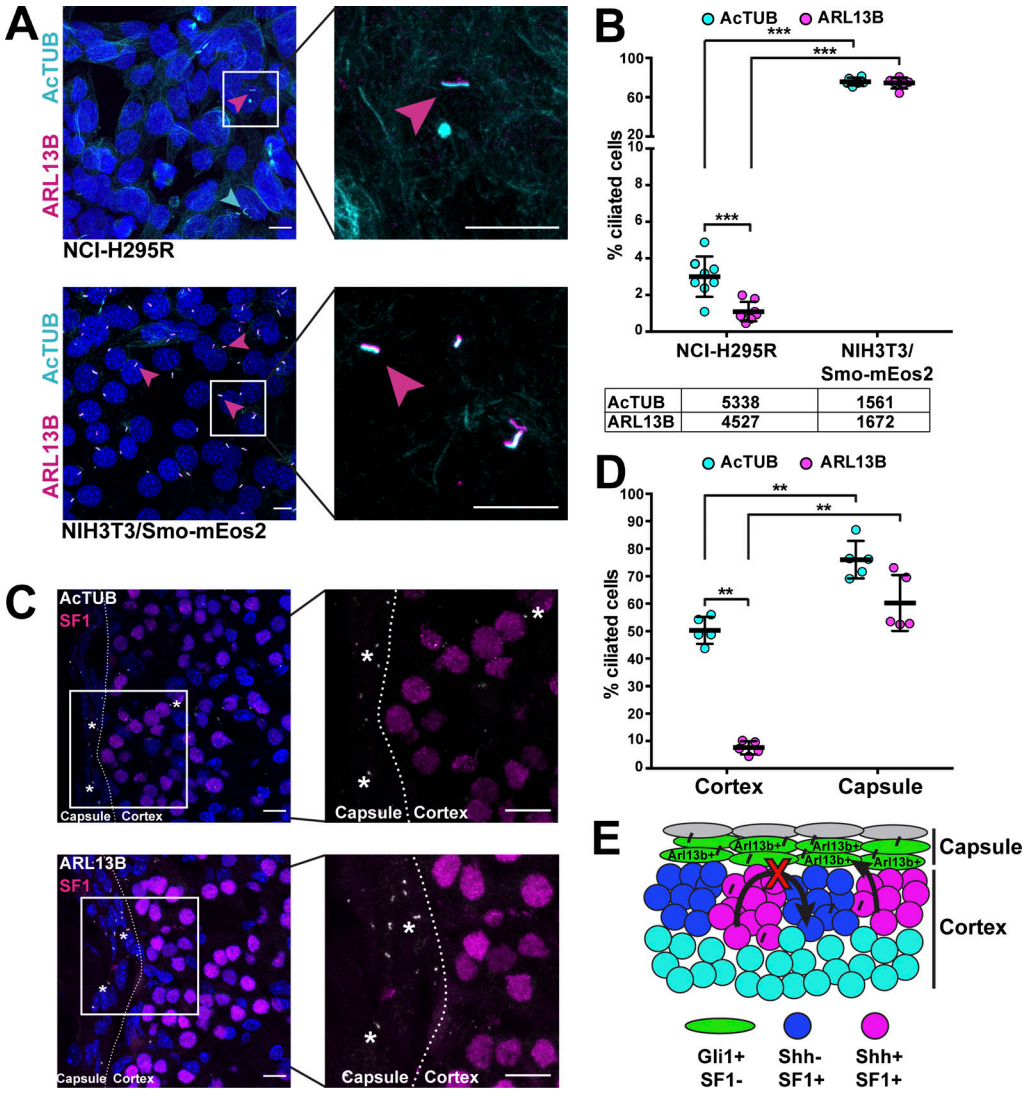

Figure 7. **Adrenocortical cells in vitro and in vivo lack ARL13B-positive primary cilia. (A)** Immunofluorescence of NCI-H295R cells (top) and NIH3T3/Smo-mEos2 cells (bottom) for acetylated tubulin (AcTUB; cyan), ARL13B (magenta), and nuclear DAPI (blue). The cyan arrowhead denotes an AcTUB-positive cilium, while the magenta arrowhead denotes a cilium where ARL13B colocalizes with AcTUB. Scale bar, 10 µm. **(B)** Quantification of the percentage of ciliated NCI-H295R and NIH3T3/Smo-mEos2 cells, counted as cells positive for AcTUB or ARL13B. The number of counted cells is given under the graph. Data are presented as mean ± SD, n = 6–8 replicates, pooled from three experiments. ***, P < 0.001. **(C)** Mouse adrenal immunofluorescence of AcTUB (top) and ARL13B (bottom), costained with SF1, a nuclear steroidogenic marker (magenta), and nuclear DAPI (blue). The dashed line represents the approximate border between the adrenal capsule and cortex. Cilia are indicated by an asterisk. Scale bar, 10 µm. **(D)** Quantification of the percentage of ciliated cells within the adrenal cortex and capsule, counted as cells positive for AcTUB or ARL13B. Each data point represents the quantification for one adrenal gland, presented as mean ± SD. **, P < 0.01. **(E)** Model representing the SHH-producing cortical and SHH-responding capsule cells in the adrenal gland. Subset of subcapsular cortical cells produce SHH (magenta) and signal to the overlying capsule cells (green), which possess ARL13B-positive primary cilia and respond by *Gli1* expression. The cortical cells themselves (magenta and blue) do not respond to autocrine SHH signaling, possibly because of a lack of ARL13B-positive cilia.

activation (Huangfu and Anderson, 2005). It is known that many solid tumors lose their primary cilia (Seeger-Nukpezah et al., 2013). Similarly, we found that only 1–5% of NCI-H295R cells are ciliated, compared with >60% of NIH3T3 fibroblasts, which respond to SHH (Fig. 7, A and B; and Fig. S4). Furthermore, only 0.5–2% of NCI-H295R cells are positive for ARL13B (Fig. 7 B and Fig. S4), a ciliary protein influencing the trafficking of SHH pathway components PTCH1, SMO, GLI2, and GLI3 (Caspary et al., 2007; Larkins et al., 2011).

This result made us wonder about the extent of ciliation in the normal adrenal gland. We found that cortical SF1-positive steroidogenic cells, which produce but do not respond to SHH (King et al., 2009), have less cilia than the overlying capsule cells, which respond to SHH (Fig. 7, C and D). Furthermore, the ciliary protein ARL13B is significantly less abundant in the cortical cells than in the capsule cells (Fig. 7, C and D). These results indicate that the inability of the cells of the adrenal cortex to respond to the autocrine SHH signal correlates with the lack of ARL13B in these cells, thus limiting the SHH response to the overlying capsular cells (Fig. 7 E). The adrenal gland also has vascular endothelial cells lying in close proximity to SHH-producing cortical cells (Bassett and West, 1997). The almost

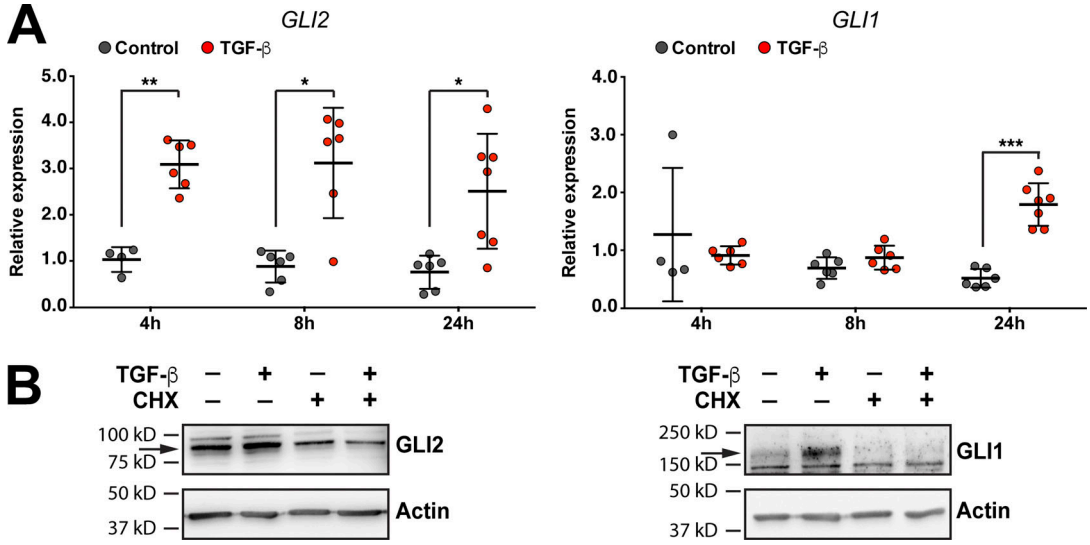

Figure 8. **TGF-β enhances *GLI2* and *GLI1* expression in human adrenocortical carcinoma cells. (A)** NCI-H295R cells were treated with 10 ng/ml TGF-β for 4, 8, and 24 h and *GLI2* and *GLI1* expression was analyzed by quantitative RT-PCR using *18S* rRNA as an internal control. Data are presented as mean ± SD, *n* = 4–6 replicates, pooled from two experiments. *, P < 0.05; **, P < 0.01; ***, P < 0.001. **(B)** Western blots of lysates from NCI-H295R cells probed for GLI1 and GLI2 (and ACTIN as a loading control), after treatment with 10 ng/ml TGF-β and 50 µg/ml cycloheximide (CHX) for 48 h. The arrows indicate the bands of GLI2 and GLI1.

complete absence of ARL13B staining in the cortex of mouse adrenal gland (Fig. 7 C) suggests that endothelial cells of the adrenal cortex are also not ciliated. Similar to adrenocortical cells, we found that only 0.95% of human umbilical vein endothelial cells (HUVECs) are ciliated (Fig. S5 A), and treatment with SAG does not induce canonical SHH signaling (Fig. S5 B).

Collectively, our data are consistent with a model in which subcapsular SHH-producing cells signal by direct contact to the overlying capsule, while the inability to respond to SHH of steroidogenic cells themselves and endothelial cells within the adrenal cortex associates with lack of the ciliary protein ARL13B in these cells (Fig. 7 E). Thus, the limited range of SHH signaling in the adrenal gland can be explained both by the physical contact between producing and receiving cells and by the presence of ARL13B-positive primary cilia in the receiving cells.

Adrenocortical carcinoma cells express *GLI2* and *GLI1* in response to TGF-β

We have seen that the adrenocortical carcinoma cells express the SHH target gene *GLI1* (Fig. 6, B and C) without responding to the SHH ligand or SMO activation (Fig. 6, E and F), highlighting a key difference between the normal and cancerous adrenocortical tissue. How, then, is SHH target gene expression ectopically produced in these cancer cells? Interestingly, another canonical target gene of the SHH pathway, *GLI2*, can be activated in normal and cancer cell types as an output of the TGF-β pathway, in a SHH-independent manner (Dennler et al., 2007). We tested whether the same crosstalk occurs in adrenocortical carcinoma cells and found that treatment of NCI-H295R cells with TGF-β rapidly increases *GLI2* expression, followed by delayed increase of *GLI1* expression (Fig. 8 A), while blocking translation abrogates the TGF-β–induced increase in GLI2 and GLI1 protein levels (Fig. 8 B). This result suggests that the expression of *GLI1* and *GLI2* is inducible in adrenocortical carcinoma cells and might be sustained at high levels by autocrine TGF-β signaling, as previously shown in pancreatic cancer cell lines (Dennler et al., 2007). Notably, in the normal murine adrenal cortex, *Shh*, *Smo*, and *Ptch1* are expressed, but *Gli1* and *Gli2* are not (Fig. 6 B), suggesting that this TGF-β–mediated pathway is not active in noncancerous adrenocortical tissue. Hence, despite the presence of SHH in both normal and cancer adrenocortical cells, the Gli-dependent Hh pathway is activated in the cancer cells only by TGF-β and not by SHH.

Discussion

Here, we use the adrenal gland to probe mechanisms limiting SHH signaling to a specific subset of receiving cells in an adult, vertebrate organ. We verify that the adrenal gland and its derived adrenocortical carcinoma cell line, NCI-H295R, share the same mechanism of secreting SHH on lipoproteins. Our data extend the existing knowledge on short- and long-range signaling of an endogenously produced mammalian SHH and allow us to make novel predictions about how the SHH pathway can be mediated in a specific, short-range pattern in the healthy adrenal gland, and how its regulation can be evaded in cancer.

While SHH signaling is predominantly short-range in the adrenal gland (Guasti et al., 2011; Laufer et al., 2012), we observe that adrenocortical cells can in fact secrete SHH on lipoproteins, which are well known to facilitate long-range morphogen transport in the *Drosophila* wing disc and developing mammalian neural tube (Eaton, 2008; Briscoe and Thérond, 2013). Specifically, we present data suggesting that SHH can associate with APOA1- and APOE-positive lipoproteins. However, further experiments are required to verify a direct interaction between them. We cannot exclude the possibility of additional

mechanisms for SHH release and transport, including on other lipoproteins like APOB-positive LDL, as proposed in other systems (Thérond, 2012; Palm et al., 2013). In conjunction, the SHH-producing cells also secrete an inhibitor that prevents SMO activation and could thereby limit the signaling range of this SHH form. Endocannabinoid lipids are likely candidates, as they were identified in both human and *Drosophila* lipoproteins and found to repress the Hh pathway in the absence of ligand (Khaliullina et al., 2015). Along these lines, we show here that N-acyldopamine 18:1 and 20:4 can inhibit the activity of HEK-ShhNc. Furthermore, we detected dopamine, the likely precursor of conjugated dopamines, by liquid chromatography–multiple reaction monitoring (LC-MRM) analysis of supernatants from mouse adrenal glands. However, under these sample preparation and analytical conditions, we could only detect a trace amount of N-acyldopamine 20:4 (data not shown); therefore, an unambiguous determination of N-acyldopamines production by mouse adrenal glands requires further investigation. It is possible that other endocannabinoids or lipoprotein-associated molecules released from adrenal gland tissue might also contribute to the inhibition of the SHH pathway.

The inability of the lipoprotein-associated SHH to signal in culture is consistent with the observation that only short-range signaling is observed in the adrenal gland. Nonetheless, we cannot rule out the possibility that the secreted form is active in vivo. Heparan sulfate proteoglycans are components of the extracellular matrix that affect SHH signaling in the lung and other tissues (Häcker et al., 2005; Zhang et al., 2007; He et al., 2017). It remains an open question whether heparan sulfate proteoglycans can interact with SHH in the adrenal gland, and whether they can locally increase the concentration of lipoprotein-associated SHH to counteract inhibitors and induce pathway activation. We predict, however, that even if this is the case, pathway activation will only be at short range, at least in the healthy adult adrenal gland.

Our observation that membrane-bound SHH can generate a response in co-cultured fibroblasts is consistent with cell-to-cell contact–mediated short-range signaling in the adrenal gland. It was previously reported that Hh pathway components transit to responding cells via membrane protrusions extending for several cell diameters from producing cells (Bischoff et al., 2013; Sanders et al., 2013; Gradilla et al., 2014; Chen et al., 2017; González-Méndez et al., 2017). Whether similar protrusions exist in the adrenal gland is unknown. Filopodia have been observed in the rat adrenal cortex and in adrenocortical cancer cells, where they were thought to be involved in steroid hormone secretion (Pudney et al., 1981; Matsuo and Tsuchiyama, 1987). Given our data, the possibility that filopodia may connect the SHH-producing and -receiving cells should also be considered.

The way adrenocortical carcinoma cells signal to neighboring fibroblasts in our co-culture system resembles the ligand-dependent paracrine signaling in many tumors between the SHH-producing cancer cells and the surrounding stromal cells (Yauch et al., 2008). SHH pathway activation in the untransformed stromal tissue elicits changes that can both positively and negatively influence tumor growth (Shaw et al., 2009; Shin et al., 2014). For example, SHH produced by hepatocellular carcinoma cells induces glycolytic changes in the surrounding stroma, thereby creating a microenvironment favoring tumor growth (Chan et al., 2012). Several groups have suggested contact-dependent SHH signal transduction in these cases (Zunich et al., 2009; Damhofer et al., 2015). In other organs, like the mouse notochord, long-range or membrane-to-membrane SHH signaling is determined by the localized expression of *Disp1*, a transmembrane protein required for secretion of cholesterol-modified SHH (Caspary et al., 2002).

While it has been suggested that activation of the Hh pathway in adrenocortical cells could be involved in tumorigenesis and that these tumors rely on SHH for growth (Boulkroun et al., 2011; Gomes et al., 2014; Werminghaus et al., 2014), we see that NCI-H295R cells are completely unresponsive to both the SHH signal itself and the SMO agonist. Thus, although adrenocortical carcinoma cells can produce SHH, they cannot respond to it and do not require it for their growth. We find that these cells express the pathway transducers *PTCH1* and *SMO*; however, they do not have cilia and lack the ciliary protein ARL13B. Primary cilia are critically important for SHH signaling (Bangs and Anderson, 2017), and the atypical GTPase ARL13B is required for maintaining ciliary structure, proper levels of GLI2/3 activator forms, and ciliary trafficking of Hh pathway components (Caspary et al., 2007; Larkins et al., 2011; Mariani et al., 2016; Revenkova et al., 2018). Thus, the low level of ciliation of adrenocortical carcinoma cells provides an explanation for the complete lack of SHH response in these cells and is consistent with the fact that many solid tumors lose their primary cilia (Seeger-Nukpezah et al., 2013).

Our results in the cancer cell line led us to propose that the cell-specific presence of the ciliary protein ARL13B could also explain the pattern of SHH response in the adrenal gland. Indeed, our data show that cells of the adrenal cortex are less ciliated than the capsule cells and that few adrenocortical cells are positive for ARL13B. SHH produced by cortical cells would thereby affect proliferation, differentiation, and *Gli1* and *Ptch1* expression only in ARL13B-positive capsular progenitors and not in cortical steroidogenic lineages (King et al., 2009; Wood and Hammer, 2011; Laufer et al., 2012). In the developing mouse neural tube, loss of ARL13B results in low-level, ligand-independent, constitutive SHH pathway activation (Caspary et al., 2007). Furthermore, it is shown that ARL13B can function outside of the cilium to regulate canonical and noncanonical SHH signaling (Mariani et al., 2016; Ferent et al., 2019; Gigante et al., 2020). In our data, the almost complete absence of GLI1-3 correlates with the absence of ciliary ARL13B in the mouse adrenal cortex. However, we cannot rule out the possibility that, due to technical limitations, we do not detect low levels of nonciliary ARL13B in our assays. It is also possible that additional mechanisms and ciliary proteins other than ARL13B might contribute to the establishment of the specific pattern of SHH signaling observed in the adrenal gland.

Unlike the normal adrenal glands, the NCI-H295R carcinoma cells constitutively express the canonical SHH target genes *GLI1* and *GLI2*. How do NCI-H295R cells express these targets if they cannot respond to SHH? We find that adrenocortical carcinoma cells behave as many other cancer cell types, by responding to TGF-β (Dennler et al., 2007; Alexaki et al., 2010; Javelaud et al.,

2011), perhaps representing an adaptive strategy for adrenocortical cancer cells to activate the mitogenic response downstream of GLI2, even though they have lost their cilia. Our results suggest that therapeutic strategies to inhibit GLI-driven tumorigenesis in adrenocortical carcinoma may benefit from targeting TGF-β rather than SHH signaling. *TGF-β* expression is considerably higher in adrenocortical cancer cells than in the normal adrenal cortex (data not shown); thus, autocrine TGF-β signaling might sustain high *GLI1* and *GLI2* expression levels. Interestingly, TGF-β was reported to reduce the expression of the steroidogenic marker SF1 in a Y-1 mouse adrenocortical cell line (Lehmann et al., 2005), suggesting that TGF-β might dedifferentiate steroidogenic adrenocortical cells while enhancing their GLI2-dependent tumorigenic potential.

Finally, in many other adult organs, the Hh pathway is a key regulator of tissue homeostatic maintenance that becomes upregulated upon injury and repair (Petrova and Joyner, 2014). Therefore, we expect that the mechanisms regulating the range of SHH pathway activity described here for the adrenal gland may also be relevant for these tissues, as SHH-producing cells are often located in distinct subregions at a short distance from the SHH-responding cells (Petrova and Joyner, 2014). Thus, this work should advance our understanding of SHH-mediated regulation of adult tissue homeostasis.

Materials and methods

Animal experiments

Wild-type C57BL/6J mice were from Harlan Laboratories or in-house husbandry of the Biomedical Services Facility (Max Planck Institute of Molecular Cell Biology and Genetics [MPI-CBG], Dresden, Germany). Heterozygous Gli^{LacZ} (Gli1tm2Alj/J) and Shh^{GFP} (Shhtm6Amc/J) mice were obtained from the Jackson Laboratory and were backcrossed to a C57BL/6J background at the Biomedical Services facility for three generations. For the HFD–induced obesity experiment, 8-wk-old mice were fed a HFD or a normal diet (60% kcal from fat or 10% kcal from fat, respectively; Research Diets Inc.) for 18 wk. After euthanasia, adrenal glands were excised in ice-cold PBS and cleaned from the surrounding fat tissue. Animal work was approved by the Ethical Committee of the Landesdirektion Dresden.

Laser microdissection of adrenal cortex

Adrenal glands from C57BL/6 mice were embedded in O.C.T. Compound (Tissue-Tek), and 25-µm-thick slices were cut with a cryotome (Cryostat NX50; Thermo Fisher Scientific) and transferred onto MembraneSlide 1.0 PEN (Zeiss). The adrenal cortex, without inclusion or disruption of the adrenal capsule, was then microdissected using a WF Laser Microdissection system (Zeiss) and the Axiovision software.

Lipoprotein isolation from plasma and serum

Human serum from human male AB plasma was purchased from Sigma-Aldrich. Mouse serum was obtained by letting mouse blood coagulate at RT, followed by centrifugation at 1,500 *g* for 20 min at 4°C. The total lipoprotein fraction was separated according to Rudel et al. (1974). A serum aliquot was adjusted to d = 1.225 g/ml with solid KBr (Sigma-Aldrich) in PBS (0.385 g KBr/ml serum solution) and centrifuged at 39,800 rpm for 24 h at 8°C in a Sw40Ti rotor (Beckman Coulter). The upper lipoprotein layer (~1 ml) was collected and desalted three times with 10 ml PBS and concentrated using an Amicon Ultra 10K (Merck Millipore).

Isolation of nonmembrane-associated SHH from adrenal glands

Adrenal glands from 30 wild-type mice were pooled together to obtain enough SHH protein to be detected by Western blotting. The glands were incubated in hyperosmotic NaCl buffer (0.5 M NaCl, 20 mM Tris-HCl, pH 8.0 [Sigma Life Science], 0.05% NP-40 [Fluka], and cOmplete Protease Inhibitor Cocktail [Roche]) for 20 min on ice, and the tissue was gently dissociated in a Dounce tissue grinder with a loose pestle on ice. The dissociated adrenals were first centrifuged at 1,000 *g* for 20 min at 4°C to obtain S1 supernatant and P1 pellet (nuclei, cell debris, and large membrane fragments were pelleted). An S1 aliquot was further centrifuged at 16,000 *g* for 20 min at 4°C to obtain S16 supernatant and P16 pellet. Last, an S16 aliquot was centrifuged at 50,000 rpm (~150,000 *g*) for 2 h at 4°C in a TLA-55 rotor (Beckman Coulter) to obtain S150 supernatant and P150 pellet (small vesicles, exosomes, and some lipoproteins were pelleted). Equal volumes of the supernatants were centrifuged at each speed, and the resulting pellets were completely dissolved in radioimmunoprecipitation assay buffer (150 mM NaCl, 0.1% Triton X-100 [Serva], 0.5% sodium deoxycholate [Sigma-Aldrich], 0.1% SDS [Serva], 50 mM Tris-HCl, pH 8.0, and cOmplete Protease Inhibitor Cocktail) in volumes equal to the volume of the corresponding supernatant. The resulting supernatants (S1, S16, and S150) were fractionated by OptiPrep density gradient centrifugation or analyzed by Western blotting.

Cell culture

NCI-H295R cells were maintained in DMEM/F-12 with L-glutamine and 15 mM Hepes (Gibco), with 2.5% Nu-Serum type 1 (BD Biosciences), 1% insulin-transferrin-selenium (ITS; Gibco), and 50 U/ml penicillin and 50 µg/ml streptomycin (Gibco), at 37°C in 5% CO_2. Nu-Serum type 1 is a serum supplement that contains 25% FBS.

HeLa and HEK-293 cells were maintained in DMEM high-glucose (Gibco) with 10% FBS (Gibco) and 50 U/ml penicillin and 50 µg/ml streptomycin, at 37°C in 5% CO_2.

Shh-LIGHT2 cells were maintained in DMEM high-glucose supplemented with 10% FBS, 150 µg/ml zeocin (Invitrogen), and 400 µg/ml geneticin (G418; Invitrogen), at 37°C in 5% CO_2. The Shh-LIGHT2 cells are NIH3T3 mouse fibroblasts, expressing a *firefly luciferase* under the control of a promoter consisting of eight consecutive Gli1-binding sites and a *Renilla luciferase* as an internal control (Sasaki et al., 1997; Taipale et al., 2000).

NIH3T3/Smo-mEos2 cells were maintained in DMEM high-glucose supplemented with 10% FCS (Gibco), 1% MEM Non-Essential Amino Acids Solution (Gibco), and 50 U/ml penicillin and 50 µg/ml streptomycin, at 37°C in 5% CO_2. The NIH3T3/Smo-mEos2 cells are NIH3T3 cells stably transfected with a construct containing the fluorescent protein mEos2 (with peak

excitation at 506 nm and peak emission at 519 nm) fused to the C terminus of SMO (Kim et al., 2014).

HUVECs (Lonza) were cultured on 0.2% gelatin-coated plates in Endothelial Cell Growth Basal Medium-2 (Lonza) supplemented with Endothelial Cell Growth Medium-2 (Lonza) at 37°C in 5% CO_2. For stimulations and ciliation, HUVECs were treated in serum-free Endothelial Cell Growth Basal Medium-2 for 24 h.

For primary adrenal cell culture, both adrenal glands from one mouse were collected in ice-cold PBS and 0.5% BSA (Sigma-Aldrich) and cleaned from the surrounding fat tissue. The adrenals were digested in a solution of 1.6 mg/ml Collagenase I (Sigma-Aldrich) and 1.6 mg/ml BSA dissolved in PBS for 1 h at 37°C in thermomixer at 900 rpm. After digestion, cells were dissociated by passing through a 22-gauge needle and 100-µm cell strainer; centrifuged at 300 *g* for 5 min at 4°C; resuspended in DMEM/F12 supplemented with 1% FBS, 50 U/ml penicillin, and 50 µg/ml streptomycin; and plated in a 96-well plate coated with 0.2% gelatin (resulting in cells from one adrenal gland per well). After 24 h, the culture supernatant was collected and centrifuged at 1,000 *g* for 20 min at 4°C.

TGF-β treatment

NCI-H295R cells were plated at 500,000 cells/well in a six-well plate. At ∼80% confluence they were stimulated with 10 ng/ml human recombinant TGF-β1 or vehicle control. After the appropriate time of culture, cells were lysed for mRNA isolation or for Western blotting. Where indicated, 50 µg/ml cycloheximide was added 30 min before TGF-β and was present throughout the whole treatment period.

Preparation of SHH-containing conditioned media

To study SHH secretion from NCI-H295R cells, cells were switched overnight to serum-free medium (DMEM/F-12 and 1% ITS), and then to serum-free medium with the appropriate serum supplement added. The resulting conditioned media were collected after 72 h, centrifuged at 1,000 *g* for 20 min at 4°C, and concentrated using an Amicon Ultra 10K for density gradient centrifugation, immunoprecipitation, or Western blotting. To prepare secreted SHH for signaling assays, the conditioned media from NCI-H295R cells grown in the appropriate experimental condition were concentrated 100× through Amicon Ultra 10K, 30K, or 100K. Controls were identically processed supplemented media without cultured cells.

To prepare lipoprotein-associated ShhNc, we used HEK-293 cells stably transfected with *SHH* or HeLa cells. HeLa cells were transfected with pCMV-XL5 plasmid encoding full-length human SHH (SC300021; OriGene) using polyethylenimine (Polysciences) in serum-free DMEM medium, switched to DMEM and 10% FBS at 6 h after transfection, and cultured for an additional 72 h. The resulting conditioned media were centrifuged at 1,000 *g* for 20 min at 4°C, and the lipoprotein-associated SHH was isolated by KBr density centrifugation (Rudel et al., 1974) and concentrated using an Amicon Ultra 10K. The controls were identically processed media from nontransfected cells.

OptiPrep density gradient centrifugation

OptiPrep density gradient centrifugation was performed according to Eugster et al. (2007). Samples were mixed with 60% OptiPrep stock solution (Sigma-Aldrich) to a final concentration of 50% OptiPrep and 45%, 35%, 25%, and 10% OptiPrep solutions were subsequently layered on top of the sample. The samples were centrifuged at 50,000 rpm for 20 h at 4°C in a TLS-55 rotor (Beckman Coulter). Fractions of 100 µl (for gradients from adrenal glands supernatants) or 200 µl (for gradients from NCI-H295R–conditioned media) were collected, and their densities were calculated based on the measured refractive index. Fractions for Western blotting were precipitated with methanol (VWR Chemicals)/chloroform (Sigma-Aldrich) and resuspended in 1× Reducing Laemmli buffer.

SDS-PAGE and Western blotting

Total protein concentration was measured using the Pierce BCA Protein Assay Kit (Thermo Fisher Scientific), according to the manufacturer's protocol. For Western blotting of cell lysates, cells were lysed either with 50 mM Tris-HCl, pH 7.4, 0.5 M NaCl, and 1% Triton X-100 (for blotting proteins with a molecular weight below 80 kD) or with 10 mM Tris-HCl, pH 7.4, 1% SDS, and 1 mM sodium vanadate (for blotting proteins with a molecular weight above 80 kD). The cell lysates were centrifuged at 16,000 *g* for 5 min at 4°C. The cell supernatants were collected and prepared for Western blotting with 5× Reducing Laemmli buffer (63 mM Tris-HCl, pH 6.8, 0.0005% bromophenol blue [Serva], 10% glycerol [Merck], 2% SDS, and 0.1% 2-mercaptoethanol [Sigma-Aldrich]). 50 µg protein were loaded in each lane.

Gel electrophoresis was performed according to standard protocols (Laemmli, 1970). Protein samples were denatured at 95°C for 5 min and loaded on a 15% acrylamide gel (Severn Biotech Ltd.) or a gradient 4–20% polyacrylamide gel (Anamed GmbH) for SDS-PAGE. SeeBlue Plus2 Pre-Stained Standard (Life Technologies) or PageRuler Prestained Protein Ladder (Thermo Fisher Scientific) was used as a protein size ladder. The separated proteins were transferred onto Amersham Protran nitrocellulose membrane (GE Healthcare Lifescience), and the transfer efficiency was estimated by staining the proteins with 0.2% Ponceau S solution (Serva). After washing in distilled water, the membranes were blocked with 5% skimmed milk in 0.1% Tween-20 (Sigma-Aldrich) in 1× TBS (TBS-T) for 1 h at RT, and washed subsequently in TBS-T. The primary antibodies were diluted in 5% BSA in TBS-T and incubated overnight at 4°C on a shaking platform, while the secondary antibodies were diluted in 5% skimmed milk in TBS-T and incubated for 1–2 h at RT. All antibodies are listed in Table 1 (primary antibodies) and Table 2 (secondary antibodies). After washing the membranes in TBS-T, the signal was detected using the SuperSignal West Pico Chemiluminiscent Substrate (Thermo Fisher Scientific) and a chemiluminiscence film (Amersham Hyperfilm ECL; GE Healthcare).

For reprobing the same membrane for multiple proteins, the membranes were stripped for 20 min at RT in stripping buffer (25 mM glycine and 1% SDS in distilled water, pH 2.2), extensively washed in TBS-T, and blocked with 5% skimmed milk in TBS-T for 30 min at RT before incubating with the next primary antibody.

Co-immunoprecipitation

The immunoprecipitation of apolipoproteins was performed using Protein-G agarose (Roche) according to the manufacturer's

Table 1. **Primary antibodies**

Antibody	Source	Dilution	Manufacturer	Use
Actin	Mouse	1:1,000	Sigma-Aldrich	WB
Acetylated tubulin	Mouse	1:1,000	Sigma-Aldrich	ICC
Acetylated tubulin	Rabbit	1:1,000	Abcam	IHC
ApoA1	Goat	1:1,000	Abcam	WB, IP
ApoA1	Rabbit	1:1,000	Calbiochem	WB
ApoE	Goat	1:500	Santa Cruz	WB, IP
ApoE	Mouse	1:500	Calbiochem	WB
Arl13b	Mouse	1:1,000	Abcam	ICC
Arl13b	Rabbit	1:500	Abcam	ICC, IHC
β-Galactosidase	Chicken	1:1,000	Abcam	IHC
GFP	Rabbit	1:500	Life Technologies	IHC
Gli1	Rabbit	1:500	Abcam	WB
Gli2	Rabbit	1:1,000	Proteintech	WB
Gli3	Goat	1:100	R&D Systems	WB
Glutamylated tubulin	Mouse	1:1,000	Adipogen	ICC
IFT88	Rabbit	1:500	Merck Millipore	ICC
PTCH1	Rat	1:500	R&D Systems	WB
SF1	Rat	1:500	TransGenic Inc.	IHC
Smoothened	Rabbit	1:500	Abcam	WB
Shh	Mouse	1:500	Invitrogen	WB
Shh	Rabbit	1:500	Cell Signaling	WB
StAR	Rabbit	1:500	Santa Cruz	ICC

ICC, immunocytochemistry; IHC, immunohistochemistry; IP, immunoprecipitation; WB, Western blotting.

protocol. The NCI-H295R–conditioned medium was adjusted with 1 M Tris-HCl, pH 7.4, to a final concentration of 50 mM Tris-HCl. To reduce the nonspecific binding to the agarose beads, the medium was first incubated with Protein-G agarose for 3 h at 4°C on rotating wheel. Beads were pelleted at 12,000 *g* and discarded. An aliquot of the supernatant was left as an input sample, and the rest was incubated with Protein-G agarose and 5 µg/ml antibody overnight at 4°C on a rotating wheel. The antibodies used are listed in Table 1. The beads were pelleted at 12,000 *g*, and the supernatant was kept as the flow-through. The beads were then washed with 50 mM Tris-HCl, pH 7.4, with increasing concentrations of NaCl—two washes with 150 mM NaCl, two washes with 0.5 M NaCl, and the last wash without NaCl—and the bound proteins were eluted by boiling the beads for 5 min in 5× non-reducing Laemmli buffer. The input and flow-through samples were precipitated with methanol/chloroform and resuspended in 1× reducing Laemmli buffer, and all samples were analyzed by Western blotting. The resulting blots were probed for SHH and the respective immunoprecipitated protein.

Shh-LIGHT2 activity assay

For the Shh-LIGHT2 activity assay, Shh-LIGHT2 cells were plated at 70,000 cells/well in 96-well plates, and after 24 h they were switched to DMEM and 1% ITS with the appropriate SHH-conditioned medium. Luciferase activity was measured in cell lysates after 24 h using the Dual Glo Luciferase Assay (Promega) according to the manufacturers' protocol.

For measuring Shh-LIGHT2 activity in co-culture experiments, 20,000 Shh-LIGHT2 cells were plated with 20,000 NCI-H295R cells either in direct physical contact in 96-well plates or separated in four-well culture inserts (Ibidi). After 24 h, the cultures were switched to DMEM and 1% ITS with or without human lipoproteins and stimulated as described. The luciferase activity was measured after 48 h using the Dual Glo Luciferase Assay.

Treatments were as follows: 10 µg/ml 5E1 monoclonal mouse antibody (produced by Protein Expression Facility, MPI-CBG), 10 µg/ml mouse IgG_1 Isotype Control (R&D Systems), 200 nM SMO agonist SAG (Calbiochem), 10 µM cyclopamine (Cayman Chemicals), and 10 µM ketoconazole (Sigma-Aldrich) or appropriate controls. The endocannabinoid lipids used are listed in Table 3.

For preparing adrenal homogenate, single adrenal glands were homogenized in 50 µl PBS with BioVortexer (BioSpec Products) on ice and centrifuged at 1,000 *g* for 20 min at 4°C, and the cleared homogenate was collected.

Gel filtration chromatography

NCI-H295R–conditioned medium was fractionated according to size by gel filtration chromatography on a Superdex 200 PC 3.2/

Table 2. **Secondary antibodies**

Antibody	Source	Dilution	Manufacturer	Use
Anti-mouse IgG, HRP	Goat	1:5,000	Merck Millipore	WB
Anti-rabbit IgG, HRP	Donkey	1:5,000	Merck Millipore	WB
Anti-goat IgG, HRP	Donkey	1:3,000	Merck Millipore	WB
Anti-rat IgG, HRP	Goat	1:5,000	Merck Millipore	WB
Anti-rabbit IgG, HRP	Goat	1:5,000	Jackson ImmunoResearch	WB
Anti-mouse IgG, Alexa 488	Goat	1:1,000	Life Technologies	ICC
Anti-mouse IgG, Alexa 647	Goat	1:1,000	Life Technologies	ICC
Anti-rabbit IgG, Alexa 555	Goat	1:1,000	Life Technologies	ICC
Anti-rabbit IgG, Alexa 647	Goat	1:1,000	Life Technologies	ICC, IHC
Anti-rat IgG, Alexa 555	Goat	1:1,000	Life Technologies	IHC
Anti-chicken IgG, Alexa 555	Goat	1:1,000	Life Technologies	IHC
Anti-rabbit IgG, light chain-specific, HRP conjugate	Mouse	1:5,000	Jackson ImmunoResearch	WB (co-IP control)
Protein G, HRP conjugate		1:5,000	Thermo Fisher Scientific	WB (co-IP control)

ICC, immunocytochemistry; IHC, immunohistochemistry; IP, immunoprecipitation; WB, Western blotting.

30 column (GE Healthcare). The running buffer used was PBS, 20 mM Hepes, and 150 mM NaCl, the fraction volume was 500 µl, and size standards were thyroglobulin (600 kD), immunoglobulin G (150 kD), ovalbumin (43 kD), myoglobin (15 kD), and vitamin B (0.16 kD). The fractions around each size peak were pooled together, concentrated to the initial volume loaded on the column, and probed for their activity on the Shh-LIGHT2 assay.

LC-MRM lipid analysis

Extraction and analysis of endocannabinoids, endocannabinoid homologues, dopamine, and dopamine conjugates was carried out using a previously described protocol with the slight modification of using dopamine-d4 as an internal standard and commercially available dopamine as a calibrant. The transitions for dopamines and dopamine conjugates included in the MRM assay were inferred from literature: N-acyl dopamine 18:1 (m/z 418.3 to m/z 154.1 and m/z 137.1), N-acyl dopamine 18:0 (m/z 420.3 to m/z 154.1 and m/z 137.1), N-acyl dopamine 20:4 (440.200 to m/z 154.1 and m/z 137.1), dopamine (m/z 154.00 to m/z 137.00 and to m/z 119 and 91, respectively) and dopamine d4 (m/z 158.0 to m/z 141.0 and 123.0, respectively). MRM transitions for endocannabinoid homologues were inferred from Bilgin and Shevchenko (2017).

Seahorse assay

A Seahorse XF96 Analyzer (Agilent Technologies) was used to measure extracellular acidification rate and oxygen consumption rate of NCI-H295R cells. NCI-H295R cells were plated at 80,000/well in a Seahorse 96-well plate coated with 0.2% gelatin (Sigma-Aldrich) and after 24 h starved in DMEM/F12 and 1% BSA for 5 h. Stimulations and measurements were performed in XF Base Medium according to the manufacturer's protocol.

Table 3. **Endocannabinoid lipids**

Compound name	Manufacturer	Catalog no.
2-Oleoyl glycerol (2AG 18:1)	Cayman Chemicals	16537
2-Arachidonoyl glycerol (2-AG 20:4)	Cayman Chemicals	62160
N-oleoyl dopamine (18:1)	Cayman Chemicals	10115
N-arachidonoyl dopamine (20:4)	Cayman Chemicals	90057

cAMP assay

The intracellular cAMP was measured using the Direct cAMP ELISA kit (Enzo Life Sciences) according to manufacturer's protocol. NCI-H295R cells were plated at 500,000 cells/well in a six-well plate, and at ∼80% confluence they were stimulated as described for the respective time periods. As a positive control for inducing cAMP production, we used 20 µM forskolin (Sigma-Aldrich).

Proliferation assay

Proliferation of NCI-H295R was measured using the BrdU Cell Proliferation ELISA Kit (Abcam), according to the manufacturer's protocol. NCI-H295R cells were cultured at 40,000 cells/well in a 96-well plate for 24 h and stimulated as described for 48 h, and BrdU was added in the last 24 h.

Quantitative real-time and semi-quantitative RT-PCR

For RT-PCR experiments, NCI-H295R cells were plated at 500,000 cells/well in a 24-well plate, and NIH3T3 cells were plated at 100,000 cells/well in a 24-well plate, stimulated as described after 24 h, and cultured for another 48 h. mRNA was extracted with the RNeasy Mini Kit (Qiagen), and cDNA was synthesized with M-MLV Reverse Transcription (Promega GMBH) according to the manufacturer's instructions. Gene expression was determined using the FastStart Essential DNA Green Master and the LightCycler96 System from Roche. The sequences of the used primers are listed in Table 4 (semi-quantitative RT-PCR) and Table 5 (quantitative RT-PCR). The relative expression of the genes was calculated using the ΔCt

Table 4. **Primers for semiquantitative RT-PCR**

Gene name	Sequence Fw (5′→3′)	Sequence Rev (5′→3′)	Amplicon length
Human *GAPDH*	CGACCACTTTGTCAAGCTCA	AGGGGTCTACATGGCAACTG	200 bp
Human *SHH*	TGATGAACCAGTGGCCAGG	GTGGCCATCTTCGTCCCA	62 bp
Human *SMO*	CAGTTTCAGCGGTGCCAAC	GGTGAGTGTGTGCAGCAGCT	74 bp
Human *PTCH1*	TGTTCGGCATGATGGGC	AGCGATCAGGATGACCACG	65 bp
Human *GLI1*	GGCACCATCCATTTCTACAGTG	TGCTTTCCTCCCTGATGGG	68 bp
Human *GLI2*	AGTTTGTTCTCGGGTGCTCTG	ACATCTGTCATCTGAAGCGGC	339 bp
Human *GLI3*	CACCCTCCTCATCTTTTCCC	GGTGTGGGGAGATCCTAATG	172 bp
Human *SUFU*	TTTACCCTGACCAGCCGAAC	TGGAACACGTATCGTGCCAA	319 bp
Mouse *Gapdh*	TCCACCACCCTGTTGCTGTA	GACTTCAACAGCAACTCCCAC	118 bp
Mouse *Shh*	CAGCGGCAGATATGAAGGGA	GGTGATGTCCACTGCTCGAC	274 bp
Mouse *Smo*	GTGTGAGAATGACCGAGTGGA	GAACAGCGGGTTCTGACACT	268 bp
Mouse *Ptch1*	TGTGGCTGAGAGCGAAGTTT	AGTGCTGAGTCCAGGTGTTG	319 bp
Mouse *Gli1*	TTCCTACGGCCATCTCTCCA	AATCGAACTCCTGGCTGCAA	386 bp
Mouse *Gli2*	AGACACCAGGAGGGAAGGTA	CGAGGCTAAAGAGTCCCCTC	301 bp
Mouse *Gli3*	GCCCTCGACGTCTAGTGATG	GTTGATGTAGGGGTGTGGGG	373 bp
Mouse *Sufu*	ACAGGAACATGGGGAGTCCT	CAATGGGCACTGTCCGTAGT	465 bp

Fw, forward; Rev, reverse.

method, and the values were normalized to those for the reference gene *β-actin* or *18S*.

Immunohistochemistry

The adrenal glands were fixed in 4% PFA in PBS, extensively washed in PBS, cryopreserved in 30% sucrose (AppliChem GmbH) in PBS overnight at 4°C, embedded in Tissue Freezing Medium (Triangle Biomedical Sciences), and frozen at −80°C. Each adrenal was cut into 8-µm-thick serial sections. Before staining, adrenal sections were prewarmed at RT for 30 min, washed with PBS, permeabilized with 0.1% Triton X-100 and 5% normal goat serum (Biowest) in PBS for 20 min, treated with 0.25% glycine in PBS for 15 min to reduce the autofluorescence, and blocked for nonspecific binding in 10% BSA in PBS for 1 h at RT. Then sections were incubated overnight at 4°C with the appropriate primary antibodies, washed with PBS, and incubated for 1 h at RT with the respective secondary antibody together with DAPI (1:5,000; Roche). All antibodies and dyes were diluted in 1% BSA in PBS and are listed in Table 1 (primary antibodies) and Table 2 (secondary antibodies). After washing with PBS, cryosections were mounted in VectaShield mounting medium (Vector Labs), covered with a 0.17-mm coverglass, fixed with nail polish, and kept at 4°C until imaging.

Immunocytochemistry

For immunocytochemistry, cells were plated on 13-mm coverslips in 24-well plates, grown until confluence, and serum-starved (DMEM or DMEM/F12 and 1% ITS) for 48 h to induce ciliation. The appropriate treatments were also performed in the starvation medium. After removal of the culture medium and washes in PBS, cells were fixed in 4% PFA for 20 min, permeabilized with 0.1% Triton X-100 and 1% BSA in PBS for 20 min, and blocked with 10% BSA in PBS for 30 min at RT. Then they were incubated with primary antibody for 2 h at RT and with secondary antibody together with DAPI for 1 h at RT. All antibodies and dyes were diluted in 1% BSA in PBS and are listed in Table 1 (primary antibodies) and Table 2 (secondary antibodies). After a series of washes, coverslips were mounted on slides with VectaShield mounting medium, fixed with nail polish, and kept at 4°C until imaging.

Image acquisition and analysis

Z-optical series microscopic images were acquired at RT on the Zeiss LSM 700 inverted confocal microscope (Zeiss); illuminated with laser lines at 405 nm, 488 nm, 555 nm, and 639 nm; and detected by two photomultiplier tube detectors. A Plan-Apochromat objective with 63× magnification, 1.40 NA, and M27 thread, working with the oil immersion medium Immersol 518 F, was used. Laser power, photomultiplier gain, and pinhole size were set for each antibody individually and kept constant for all subsequent image acquisitions. For each condition, at least six view fields were imaged per coverslip or tissue section. Images were acquired with the ZEN 2012 (SP5 FP3 Black, 64-bit) software, and processed and quantified with the Fiji/ImageJ software. The quantification of cell and cilia number in cell cultures was done on maximum intensity Z-projection images with the Cell Counter plugin in Fiji. The quantification of cell and cilia number in adrenal glands sections was done with a Fiji script written by the Scientific Computing facility (MPI-CBG and Center for Systems Biology Dresden).

Statistical analysis

The statistical analysis and plotting of the results were performed with Graphpad Prism version 6.0c (GraphPad Software

Table 5. **Primers for quantitative real-time RT-PCR**

Gene name	Sequence Fw (5′→3′)	Sequence Rev (5′→3′)
Human *18S*	TGCCCTATCAACTTTCGATG	GATGTGGTAGCCGTTTCTCA
Human *B-ACTIN*	GCCGTCTTCCCCTCCATCGTG	GGAGCCACACGCAGCTCATTGTAGA
Human *PTCH1*	CCACAGAAGCGCTCCTACAA	TGTTCCAATTTCCACTGCCTG
Human *GLI1*	AGAGAGACCAACAGCTGCAC	GAGGTGAGATGGACAGTGCC
Human *GLI2*	CCCACGCTCTCCATGATCTC	AGCAGGAAGGCCAAACAGTC
Mouse *b-Actin*	GAGCACAGCTTCTTTGCAGCTCCTT	TGCCATGTTCAATGGGGTACTTCAG
Mouse *Ptch1*	TGCTGTGCCTGTGGTCATCCTGATT	CAGAGCGAGCATAGCCCTGTGGTTC
Mouse *Gli1*	CAGCAGCTGCACTGAAGGATCTC	GCTGGCATCAGAAAGGGGCG

Fw, forward; Rev, reverse.

Inc.). Data were analyzed with the Mann–Whitney *U* test and are graphically represented as mean ± SD.

Online supplemental material

Fig. S1 shows that HFD-induced obesity in mice does not change the fractionation of SHH or lipoproteins in the adrenal gland. Fig. S2 provides additional data on the inhibitory activity of NCI-H295R–derived conditioned medium on the SHH signaling activity in Shh-LIGHT2 cells. Fig. S3 shows that human adrenocortical carcinoma NCI-H295R cells do not respond to autocrine noncanonical SHH signaling. Fig. S4 provides additional data showing that NCI-H295R cells are poorly ciliated. Fig. S5 shows that HUVECs do not respond to canonical SHH signaling.

Acknowledgments

We dedicate this manuscript to our endlessly inspiring colleague and mentor, Suzanne Eaton, who sadly passed away during the last stages of its preparation.

We are grateful to Valentina Greco, Marino Zerial, Jacqueline M. Tabler, Triantafyllos Chavakis, Stefan R. Bornstein, Marta M. Swierczynska, Petra Born, Stephanie Spannl, and Suhrid Ghosh for helpful discussions and critical comments on the manuscript. We acknowledge Canelif Yilmaz for performing laser microdissection of the adrenal cortex, Christine Mund for technical assistance, and Philip Beachy (Stanford University School of Medicine, Standford, CA) for providing Shh-LIGHT2 and NIH3T3/Smo-mEos2 cells. We thank Laura Bindila (Lipidomics Unit, University Medical Center Mainz of the Johannes Gutenberg University Mainz) for performing the LC-MRM lipid analysis, Barbara Borgonovo (MPI-CBG) for assisting with gel filtration chromatography, the Biomedical Services Facility (MPI-CBG) for help with animal husbandry, the Light Microscopy Facility (MPI-CBG) for help with imaging, and the Scientific Computing Facility (MPI-CBG and Center for Systems Biology Dresden) for providing the Fiji script for cell and cilia quantification in adrenal glands.

This work was supported by grants from the Deutsche Forschungsgemeinschaft (KFO 252 and TRR83 to S. Eaton, and SFB-TRR 205 to S. Eaton and V.I. Alexaki), and by the Max Planck Gesellschaft.

The authors declare no competing financial interests.

Author contributions: Conceptualization: I. Mateska, V.I. Alexaki, and S. Eaton; Investigation: I. Mateska, K. Nanda, and V.I. Alexaki; Formal Analysis: I. Mateska, K. Nanda, V.I. Alexaki, and S. Eaton; Methodology: I. Mateska, V.I. Alexaki, and S. Eaton; Visualization: I. Mateska; Writing/Original Draft Preparation: I. Mateska, N.A. Dye, V.I. Alexaki, and S. Eaton; Writing/Review and Editing: I. Mateska, N.A. Dye, and V.I. Alexaki; Supervision: N.A. Dye, V.I. Alexaki, and S. Eaton; Funding Acquisition: V.I. Alexaki and S. Eaton.

Submitted: 22 October 2019
Revised: 27 July 2020
Accepted: 15 September 2020

References

Alexaki, V.I., D. Javelaud, L.C.L. Van Kempen, K.S. Mohammad, S. Dennler, F. Luciani, K.S. Hoek, P. Juàrez, J.S. Goydos, P.J. Fournier, et al. 2010. GLI2-mediated melanoma invasion and metastasis. *J. Natl. Cancer Inst.* 102: 1148–1159. https://doi.org/10.1093/jnci/djq257

Bangs, F., and K.V. Anderson. 2017. Primary cilia and Mammalian Hedgehog signaling. *Cold Spring Harb. Perspect. Biol.* 9:a028175. https://doi.org/10.1101/cshperspect.a028175

Bassett, J.R., and S.H. West. 1997. Vascularization of the adrenal cortex: its possible involvement in the regulation of steroid hormone release. *Microsc. Res. Tech.* 36:546–557. https://doi.org/10.1002/(SICI)1097-0029(19970315)36:6<546::AID-JEMT11>3.0.CO;2-O

Berman, D.M., S.S. Karhadkar, A. Maitra, R. Montes De Oca, M.R. Gerstenblith, K. Briggs, A.R. Parker, Y. Shimada, J.R. Eshleman, D.N. Watkins, and P.A. Beachy. 2003. Widespread requirement for Hedgehog ligand stimulation in growth of digestive tract tumours. *Nature.* 425:846–851. https://doi.org/10.1038/nature01972

Bilgin, M., and A. Shevchenko. 2017. Quantification of Endogenous Endocannabinoids by LC-MS/MS. *Lipidomics.* 125:99–107. https://doi.org/10.1007/978-1-4939-6946-3_7

Bischoff, M., A.-C. Gradilla, I. Seijo, G. Andrés, C. Rodríguez-Navas, L. González-Méndez, and I. Guerrero. 2013. Cytonemes are required for the establishment of a normal Hedgehog morphogen gradient in Drosophila epithelia. *Nat. Cell Biol.* 15:1269–1281. https://doi.org/10.1038/ncb2856

Boulkroun, S., B. Samson-Couterie, J.F. Golib-Dzib, L. Amar, P.F. Plouin, M. Sibony, H. Lefebvre, E. Louiset, X. Jeunemaitre, T. Meatchi, et al. 2011. Aldosterone-producing adenoma formation in the adrenal cortex involves expression of stem/progenitor cell markers. *Endocrinology.* 152: 4753–4763. https://doi.org/10.1210/en.2011-1205

Briscoe, J., and P.P. Thérond. 2013. The mechanisms of Hedgehog signalling and its roles in development and disease. *Nat. Rev. Mol. Cell Biol.* 14: 416–429. https://doi.org/10.1038/nrm3598

Campbell, W.B., M.T. Brady, L.J. Rosolowsky, and J.R. Falck. 1991. Metabolism of arachidonic acid by rat adrenal glomerulosa cells: synthesis of hydroxyeicosatetraenoic acids and epoxyeicosatrienoic acids. *Endocrinology*. 128:2183–2194. https://doi.org/10.1210/endo-128-4-2183

Caspary, T., M.J. García-García, D. Huangfu, J.T. Eggenschwiler, M.R. Wyler, A.S. Rakeman, H.L. Alcorn, and K.V. Anderson. 2002. Mouse Dispatched homolog1 is required for long-range, but not juxtacrine, Hh signaling. *Curr. Biol.* 12:1628–1632. https://doi.org/10.1016/S0960-9822(02)01147-8

Caspary, T., C.E. Larkins, and K.V. Anderson. 2007. The graded response to Sonic Hedgehog depends on cilia architecture. *Dev. Cell.* 12:767–778. https://doi.org/10.1016/j.devcel.2007.03.004

Chan, I.S., C.D. Guy, Y. Chen, J. Lu, M. Swiderska-Syn, G.A. Michelotti, G. Karaca, G. Xie, L. Krüger, W.K. Syn, et al. 2012. Paracrine Hedgehog signaling drives metabolic changes in hepatocellular carcinoma. *Cancer Res.* 72:6344–6350. https://doi.org/10.1158/0008-5472.CAN-12-1068

Chen, W., H. Huang, R. Hatori, and T.B. Kornberg. 2017. Essential basal cytonemes take up Hedgehog in the *Drosophila* wing imaginal disc. *Development*. 144:3134–3144. https://doi.org/10.1242/dev.149856

Ching, S., and E. Vilain. 2009. Targeted disruption of Sonic Hedgehog in the mouse adrenal leads to adrenocortical hypoplasia. *Genesis*. 47:628–637. https://doi.org/10.1002/dvg.20532

Christensen, S.T., L.B. Pedersen, L. Schneider, and P. Satir. 2007. Sensory cilia and integration of signal transduction in human health and disease. *Traffic*. 8:97–109. https://doi.org/10.1111/j.1600-0854.2006.00516.x

Corbit, K.C., P. Aanstad, V. Singla, A.R. Norman, D.Y.R. Stainier, and J.F. Reiter. 2005. Vertebrate Smoothened functions at the primary cilium. *Nature*. 437:1018–1021. https://doi.org/10.1038/nature04117

Damhofer, H., V.L. Veenstra, J.A.M.G. Tol, H.W.M. van Laarhoven, J.P. Medema, and M.F. Bijlsma. 2015. Blocking Hedgehog release from pancreatic cancer cells increases paracrine signaling potency. *J. Cell Sci.* 128:129–139. https://doi.org/10.1242/jcs.157966

Dennler, S., J. André, I. Alexaki, A. Li, T. Magnaldo, P. ten Dijke, X.J. Wang, F. Verrecchia, and A. Mauviel. 2007. Induction of sonic hedgehog mediators by transforming growth factor-β: Smad3-dependent activation of Gli2 and Gli1 expression in vitro and in vivo. *Cancer Res.* 67:6981–6986. https://doi.org/10.1158/0008-5472.CAN-07-0491

Eaton, S. 2008. Multiple roles for lipids in the Hedgehog signalling pathway. *Nat. Rev. Mol. Cell Biol.* 9:437–445. https://doi.org/10.1038/nrm2414

Eugster, C., D. Panáková, A. Mahmoud, and S. Eaton. 2007. Lipoprotein-heparan sulfate interactions in the Hh pathway. *Dev. Cell.* 13:57–71. https://doi.org/10.1016/j.devcel.2007.04.019

Ferent, J., S. Constable, E.D. Gigante, P.T. Yam, L.E. Mariani, E. Legué, K.F. Liem Jr., T. Caspary, and F. Charron. 2019. The Ciliary Protein Arl13b Functions Outside of the Primary Cilium in Shh-Mediated Axon Guidance. *Cell Rep.* 29:3356–3366.e3. https://doi.org/10.1016/j.celrep.2019.11.015

Frazier-Wood, A.C., S. Glasser, W.T. Garvey, E.K. Kabagambe, I.B. Borecki, H.K. Tiwari, M.Y. Tsai, P.N. Hopkins, J.M. Ordovas, and D.K. Arnett. 2011. A clustering analysis of lipoprotein diameters in the metabolic syndrome. *Lipids Health Dis.* 10:237. https://doi.org/10.1186/1476-511X-10-237

Freedman, B.D., P.B. Kempna, D.L. Carlone, M. Shah, N.A. Guagliardo, P.Q. Barrett, C.E. Gomez-Sanchez, J.A. Majzoub, and D.T. Breault. 2013. Adrenocortical zonation results from lineage conversion of differentiated zona glomerulosa cells. *Dev. Cell.* 26:666–673. https://doi.org/10.1016/j.devcel.2013.07.016

Gazdar, A.F., H.K. Oie, C.H. Shackleton, T.R. Chen, T.J. Triche, C.E. Myers, G.P. Chrousos, M.F. Brennan, C.A. Stein, and R.V. La Rocca. 1990. Establishment and characterization of a human adrenocortical carcinoma cell line that expresses multiple pathways of steroid biosynthesis. *Cancer Res.* 50:5488–5496.

German, J.B., J.T. Smilowitz, and A.M. Zivkovic. 2006. Lipoproteins: When size really matters. *Curr. Opin. Colloid Interface Sci.* 11:171–183. https://doi.org/10.1016/j.cocis.2005.11.006

Gigante, E.D., M.R. Taylor, A.A. Ivanova, R.A. Kahn, and T. Caspary. 2020. ARL13B regulates Sonic hedgehog signaling from outside primary cilia. *eLife*. 9:e50434. https://doi.org/10.7554/eLife.50434

Gomes, D.C., L.F. Leal, L.M. Mermejo, C.A. Scrideli, C.E. Martinelli Jr., M.C.B.V. Fragoso, A.C. Latronico, L.G. Tone, S. Tucci, J.A. Yunes, et al. 2014. Sonic hedgehog signaling is active in human adrenal cortex development and deregulated in adrenocortical tumors. *J. Clin. Endocrinol. Metab.* 99:E1209–E1216. https://doi.org/10.1210/jc.2013-4098

González-Méndez, L., I. Seijo-Barandiarán, and I. Guerrero. 2017. Cytoneme-mediated cell-cell contacts for Hedgehog reception. *eLife*. 6:e24045. https://doi.org/10.7554/eLife.24045

Gradilla, A.-C., E. González, I. Seijo, G. Andrés, M. Bischoff, L. González-Mendez, V. Sánchez, A. Callejo, C. Ibáñez, M. Guerra, et al. 2014. Exosomes as Hedgehog carriers in cytoneme-mediated transport and secretion. *Nat. Commun.* 5:5649. https://doi.org/10.1038/ncomms6649

Guasti, L., A. Paul, E. Laufer, and P. King. 2011. Localization of Sonic hedgehog secreting and receiving cells in the developing and adult rat adrenal cortex. *Mol. Cell. Endocrinol.* 336:117–122. https://doi.org/10.1016/j.mce.2010.11.010

Häcker, U., K. Nybakken, and N. Perrimon. 2005. Heparan sulphate proteoglycans: the sweet side of development. *Nat. Rev. Mol. Cell Biol.* 6:530–541. https://doi.org/10.1038/nrm1681

Haycraft, C.J., B. Banizs, Y. Aydin-Son, Q. Zhang, E.J. Michaud, and B.K. Yoder. 2005. Gli2 and Gli3 localize to cilia and require the intraflagellar transport protein polaris for processing and function. *PLoS Genet.* 1:e53. https://doi.org/10.1371/journal.pgen.0010053

He, H., M. Huang, S. Sun, Y. Wu, and X. Lin. 2017. Epithelial heparan sulfate regulates Sonic Hedgehog signaling in lung development. *PLoS Genet.* 13:e1006992. https://doi.org/10.1371/journal.pgen.1006992

Hegele, R.A. 2009. Plasma lipoproteins: genetic influences and clinical implications. *Nat. Rev. Genet.* 10:109–121. https://doi.org/10.1038/nrg2481

Huang, C.C.J., S. Miyagawa, D. Matsumaru, K.L. Parker, and H.H.C. Yao. 2010. Progenitor cell expansion and organ size of mouse adrenal is regulated by sonic hedgehog. *Endocrinology*. 151:1119–1128. https://doi.org/10.1210/en.2009-0814

Huangfu, D., and K.V. Anderson. 2005. Cilia and Hedgehog responsiveness in the mouse. *Proc. Natl. Acad. Sci. USA*. 102:11325–11330. https://doi.org/10.1073/pnas.0505328102

Hui, C.C., and S. Angers. 2011. Gli proteins in development and disease. *Annu. Rev. Cell Dev. Biol.* 27:513–537. https://doi.org/10.1146/annurev-cellbio-092910-154048

Humke, E.W., K.V. Dorn, L. Milenkovic, M.P. Scott, and R. Rohatgi. 2010. The output of Hedgehog signaling is controlled by the dynamic association between Suppressor of Fused and the Gli proteins. *Genes Dev.* 24:670–682. https://doi.org/10.1101/gad.1902910

Igal, R.A., E.C. Mandon, and I.N. de Gómez Dumm. 1991. Abnormal metabolism of polyunsaturated fatty acids in adrenal glands of diabetic rats. *Mol. Cell. Endocrinol.* 77:217–227. https://doi.org/10.1016/0303-7207(91)90077-6

Ingham, P.W., and A.P. McMahon. 2001. Hedgehog signaling in animal development: paradigms and principles. *Genes Dev.* 15:3059–3087. https://doi.org/10.1101/gad.938601

Ingham, P.W., Y. Nakano, and C. Seger. 2011. Mechanisms and functions of Hedgehog signalling across the metazoa. *Nat. Rev. Genet.* 12:393–406. https://doi.org/10.1038/nrg2984

Javelaud, D., V.I. Alexaki, S. Dennler, K.S. Mohammad, T.A. Guise, and A. Mauviel. 2011. TGF-β/SMAD/GLI2 signaling axis in cancer progression and metastasis. *Cancer Res.* 71:5606–5610. https://doi.org/10.1158/0008-5472.CAN-11-1194

Jonas, A., and M.C. Phillips. 2008. Lipoprotein Structure. *In* Biochemistry of Lipids, Lipoproteins and Membranes. D.E. Vance, and J.E. Vance, editors. Fifth edition. Elsevier B.V. pp. 485–506.

Keegan, C.E., and G.D. Hammer. 2002. Recent insights into organogenesis of the adrenal cortex. *Trends Endocrinol. Metab.* 13:200–208. https://doi.org/10.1016/S1043-2760(02)00602-1

Khaliullina, H., D. Panáková, C. Eugster, F. Riedel, M. Carvalho, and S. Eaton. 2009. Patched regulates Smoothened trafficking using lipoprotein-derived lipids. *Development*. 136:4111–4121. https://doi.org/10.1242/dev.041392

Khaliullina, H., M. Bilgin, J.L. Sampaio, A. Shevchenko, and S. Eaton. 2015. Endocannabinoids are conserved inhibitors of the Hedgehog pathway. *Proc. Natl. Acad. Sci. USA*. 112:3415–3420. https://doi.org/10.1073/pnas.1416463112

Kim, J., E.Y.C. Hsia, J. Kim, N. Sever, P.A. Beachy, and X. Zheng. 2014. Simultaneous measurement of smoothened entry into and exit from the primary cilium. *PLoS One*. 9:e104070. https://doi.org/10.1371/journal.pone.0104070

King, P., A. Paul, and E. Laufer. 2009. Shh signaling regulates adrenocortical development and identifies progenitors of steroidogenic lineages. *Proc. Natl. Acad. Sci. USA*. 106:21185–21190. https://doi.org/10.1073/pnas.0909471106

Kornberg, T.B., and S. Roy. 2014. Cytonemes as specialized signaling filopodia. *Development*. 141:729–736. https://doi.org/10.1242/dev.086223

Kraemer, F.B. 2007. Adrenal cholesterol utilization. *Mol. Cell. Endocrinol.* 265-266:42–45. https://doi.org/10.1016/j.mce.2006.12.001

Kuwabara, P.E., and M. Labouesse. 2002. The sterol-sensing domain: multiple families, a unique role? *Trends Genet.* 18:193–201. https://doi.org/10.1016/S0168-9525(02)02640-9

Laemmli, U.K. 1970. Cleavage of structural proteins during the assembly of the head of bacteriophage T4. *Nature.* 227:680–685. https://doi.org/10.1038/227680a0

Larkins, C.E., G.D.G. Aviles, M.P. East, R.A. Kahn, and T. Caspary. 2011. Arl13b regulates ciliogenesis and the dynamic localization of Shh signaling proteins. *Mol. Biol. Cell.* 22:4694–4703. https://doi.org/10.1091/mbc.e10-12-0994

Laufer, E., D. Kesper, A. Vortkamp, and P. King. 2012. Sonic hedgehog signaling during adrenal development. *Mol. Cell. Endocrinol.* 351:19–27. https://doi.org/10.1016/j.mce.2011.10.002

Lehmann, T.P., J.M. Biernacka-Lukanty, W.H. Trzeciak, J.Y. Li, and J.Y. Li. 2005. Steroidogenic factor 1 gene transcription is inhibited by transforming growth factor β. *Endocr. Res.* 31:71–79. https://doi.org/10.1080/07435800500229110

Mariani, L.E., M.F. Bijlsma, A.A. Ivanova, S.K. Suciu, R.A. Kahn, and T. Caspary. 2016. Arl13b regulates Shh signaling from both inside and outside the cilium. *Mol. Biol. Cell.* 27:3780–3790. https://doi.org/10.1091/mbc.e16-03-0189

Matsuo, K., and H. Tsuchiyama. 1987. Human normal and neoplastic adrenocortical cells in tissue culture observed by scanning electron microscopy. *Acta Pathol. Jpn.* 37:65–76. https://doi.org/10.1111/j.1440-1827.1987.tb03134.x

Milenkovic, L., M.P. Scott, and R. Rohatgi. 2009. Lateral transport of Smoothened from the plasma membrane to the membrane of the cilium. *J. Cell Biol.* 187:365–374. https://doi.org/10.1083/jcb.200907126

Nielsen, F.K., C.H. Hansen, J.A. Fey, M. Hansen, N.W. Jacobsen, B. Halling-Sørensen, E. Björklund, and B. Styrishave. 2012. H295R cells as a model for steroidogenic disruption: a broader perspective using simultaneous chemical analysis of 7 key steroid hormones. *Toxicol. In Vitro.* 26:343–350. https://doi.org/10.1016/j.tiv.2011.12.008

Palm, W., M.M. Swierczynska, V. Kumari, M. Ehrhart-Bornstein, S.R. Bornstein, and S. Eaton. 2013. Secretion and signaling activities of lipoprotein-associated hedgehog and non-sterol-modified hedgehog in flies and mammals. *PLoS Biol.* 11:e1001505. https://doi.org/10.1371/journal.pbio.1001505

Panáková, D., H. Sprong, E. Marois, C. Thiele, and S. Eaton. 2005. Lipoprotein particles are required for Hedgehog and Wingless signalling. *Nature.* 435:58–65. https://doi.org/10.1038/nature03504

Petrova, R., and A.L. Joyner. 2014. Roles for Hedgehog signaling in adult organ homeostasis and repair. *Development.* 141:3445–3457. https://doi.org/10.1242/dev.083691

Pudney, J., P.R. Sweet, G.P. Vinson, and B.J. Whitehouse. 1981. Morphological correlates of hormone secretion in the rat adrenal cortex and the role of filopodia. *Anat. Rec.* 201:537–551. https://doi.org/10.1002/ar.1092010310

Rainey, W.E., K. Saner, and B.P. Schimmer. 2004. Adrenocortical cell lines. *Mol. Cell. Endocrinol.* 228:23–38. https://doi.org/10.1016/j.mce.2003.12.020

Revenkova, E., Q. Liu, G.L. Gusella, and C. Iomini. 2018. The Joubert syndrome protein ARL13B binds tubulin to maintain uniform distribution of proteins along the ciliary membrane. *J. Cell Sci.* 131:jcs212324. https://doi.org/10.1242/jcs.212324

Riobo, N.A., B. Saucy, C. Dilizio, and D.R. Manning. 2006. Activation of heterotrimeric G proteins by Smoothened. *Proc. Natl. Acad. Sci. USA.* 103:12607–12612. https://doi.org/10.1073/pnas.0600880103

Rohatgi, R., L. Milenkovic, and M.P. Scott. 2007. Patched1 regulates hedgehog signaling at the primary cilium. *Science.* 317:372–376. https://doi.org/10.1126/science.1139740

Rojas-Ríos, P., I. Guerrero, and A. González-Reyes. 2012. Cytoneme-mediated delivery of hedgehog regulates the expression of bone morphogenetic proteins to maintain germline stem cells in Drosophila. *PLoS Biol.* 10:e1001298. https://doi.org/10.1371/journal.pbio.1001298

Rudel, L.L., J.A. Lee, M.D. Morris, and J.M. Felts. 1974. Characterization of plasma lipoproteins separated and purified by agarose-column chromatography. *Biochem. J.* 139:89–95. https://doi.org/10.1042/bj1390089

Sanders, T.A., E. Llagostera, and M. Barna. 2013. Specialized filopodia direct long-range transport of SHH during vertebrate tissue patterning. *Nature.* 497:628–632. https://doi.org/10.1038/nature12157

Sasaki, H., C. Hui, M. Nakafuku, and H. Kondoh. 1997. A binding site for Gli proteins is essential for HNF-3β floor plate enhancer activity in transgenics and can respond to Shh in vitro. *Development.* 124:1313–1322.

Seeger-Nukpezah, T., J.L. Little, V. Serzhanova, and E.A. Golemis. 2013. Cilia and cilia-associated proteins in cancer. *Drug Discov. Today Dis. Mech.* 10:e135–e142. https://doi.org/10.1016/j.ddmec.2013.03.004

Shaw, A., J. Gipp, and W. Bushman. 2009. The Sonic Hedgehog pathway stimulates prostate tumor growth by paracrine signaling and recapitulates embryonic gene expression in tumor myofibroblasts. *Oncogene.* 28:4480–4490. https://doi.org/10.1038/onc.2009.294

Shen, F., L. Cheng, A.E. Douglas, N.A. Riobo, and D.R. Manning. 2013. Smoothened is a fully competent activator of the heterotrimeric G protein G(i). *Mol. Pharmacol.* 83:691–697. https://doi.org/10.1124/mol.112.082511

Shin, K., A. Lim, C. Zhao, D. Sahoo, Y. Pan, E. Spiekerkoetter, J.C. Liao, and P.A. Beachy. 2014. Hedgehog signaling restrains bladder cancer progression by eliciting stromal production of urothelial differentiation factors. *Cancer Cell.* 26:521–533. https://doi.org/10.1016/j.ccell.2014.09.001

Swierczynska, M.M., I. Mateska, M. Peitzsch, S.R. Bornstein, T. Chavakis, G. Eisenhofer, V. Lamounier-Zepter, and S. Eaton. 2015. Changes in morphology and function of adrenal cortex in mice fed a high-fat diet. *Int. J. Obes.* 39:321–330. https://doi.org/10.1038/ijo.2014.102

Taipale, J., J.K. Chen, M.K. Cooper, B. Wang, R.K. Mann, L. Milenkovic, M.P. Scott, and P.A. Beachy. 2000. Effects of oncogenic mutations in Smoothened and Patched can be reversed by cyclopamine. *Nature.* 406:1005–1009. https://doi.org/10.1038/35023008

Taipale, J., M.K. Cooper, T. Maiti, and P.A. Beachy. 2002. Patched acts catalytically to suppress the activity of Smoothened. *Nature.* 418:892–897. https://doi.org/10.1038/nature00989

Tanaka, Y., Y. Okada, and N. Hirokawa. 2005. FGF-induced vesicular release of Sonic hedgehog and retinoic acid in leftward nodal flow is critical for left-right determination. *Nature.* 435:172–177. https://doi.org/10.1038/nature03494

Teperino, R., S. Amann, M. Bayer, S.L. McGee, A. Loipetzberger, T. Connor, C. Jaeger, B. Kammerer, L. Winter, G. Wiche, et al. 2012. Hedgehog partial agonism drives Warburg-like metabolism in muscle and brown fat. *Cell.* 151:414–426. https://doi.org/10.1016/j.cell.2012.09.021

Teperino, R., F. Aberger, H. Esterbauer, N. Riobo, and J.A. Pospisilik. 2014. Canonical and non-canonical Hedgehog signalling and the control of metabolism. *Semin. Cell Dev. Biol.* 33:81–92. https://doi.org/10.1016/j.semcdb.2014.05.007

Thérond, P.P. 2012. Release and transportation of Hedgehog molecules. *Curr. Opin. Cell Biol.* 24:173–180. https://doi.org/10.1016/j.ceb.2012.02.001

Tukachinsky, H., L.V. Lopez, and A. Salic. 2010. A mechanism for vertebrate Hedgehog signaling: recruitment to cilia and dissociation of SuFu-Gli protein complexes. *J. Cell Biol.* 191:415–428. https://doi.org/10.1083/jcb.201004108

Vyas, N., A. Walvekar, D. Tate, V. Lakshmanan, D. Bansal, A. Lo Cicero, G. Raposo, D. Palakodeti, and J. Dhawan. 2014. Vertebrate Hedgehog is secreted on two types of extracellular vesicles with different signaling properties. *Sci. Rep.* 4:7357. https://doi.org/10.1038/srep07357

Watkins, D.N., D.M. Berman, S.G. Burkholder, B. Wang, P.A. Beachy, and S.B. Baylin. 2003. Hedgehog signalling within airway epithelial progenitors and in small-cell lung cancer. *Nature.* 422:313–317. https://doi.org/10.1038/nature01493

Werminghaus, P., M. Haase, P.J. Hornsby, S. Schinner, M. Schott, L.K. Malendowicz, B.J. Lammers, P.E. Goretzki, V. Müller-Mattheis, Markus Giessing, and H.S. Willenberg. 2014. Hedgehog-signaling is upregulated in non-producing human adrenal adenomas and antagonism of hedgehog-signaling inhibits proliferation of NCI-H295R cells and an immortalized primary human adrenal cell line. *J. Steroid Biochem. Mol. Biol.* 139:7–15. https://doi.org/10.1016/j.jsbmb.2013.09.007

Wetmore, C. 2003. Sonic hedgehog in normal and neoplastic proliferation: insight gained from human tumors and animal models. *Curr. Opin. Genet. Dev.* 13:34–42. https://doi.org/10.1016/S0959-437X(03)00002-9

Wood, M.A., and G.D. Hammer. 2011. Adrenocortical stem and progenitor cells: unifying model of two proposed origins. *Mol. Cell. Endocrinol.* 336:206–212. https://doi.org/10.1016/j.mce.2010.11.012

Yates, R., H. Katugampola, D. Cavlan, K. Cogger, E. Meimaridou, C. Hughes, L. Metherell, L. Guasti, and P. King. 2013. Adrenocortical Development, Maintenance, and Disease. *In* Curr. Top Dev. Biol. Vol. Vol. 106. P. Thomas, editor. Elsevier Inc. pp. 239–312.

Yauch, R.L., S.E. Gould, S.J. Scales, T. Tang, H. Tian, C.P. Ahn, D. Marshall, L. Fu, T. Januario, D. Kallop, et al. 2008. A paracrine requirement for hedgehog signalling in cancer. *Nature.* 455:406–410. https://doi.org/10.1038/nature07275

Zhang, F., J.S. McLellan, A.M. Ayala, D.J. Leahy, and R.J. Linhardt. 2007. Kinetic and structural studies on interactions between heparin or heparan sulfate and proteins of the hedgehog signaling pathway. *Biochemistry.* 46:3933–3941. https://doi.org/10.1021/bi6025424

Zunich, S.M., T. Douglas, M. Valdovinos, T. Chang, W. Bushman, D. Walterhouse, P. Iannaccone, and M.L.G. Lamm. 2009. Paracrine sonic hedgehog signalling by prostate cancer cells induces osteoblast differentiation. *Mol. Cancer.* 8:12. https://doi.org/10.1186/1476-4598-8-12

Supplemental material

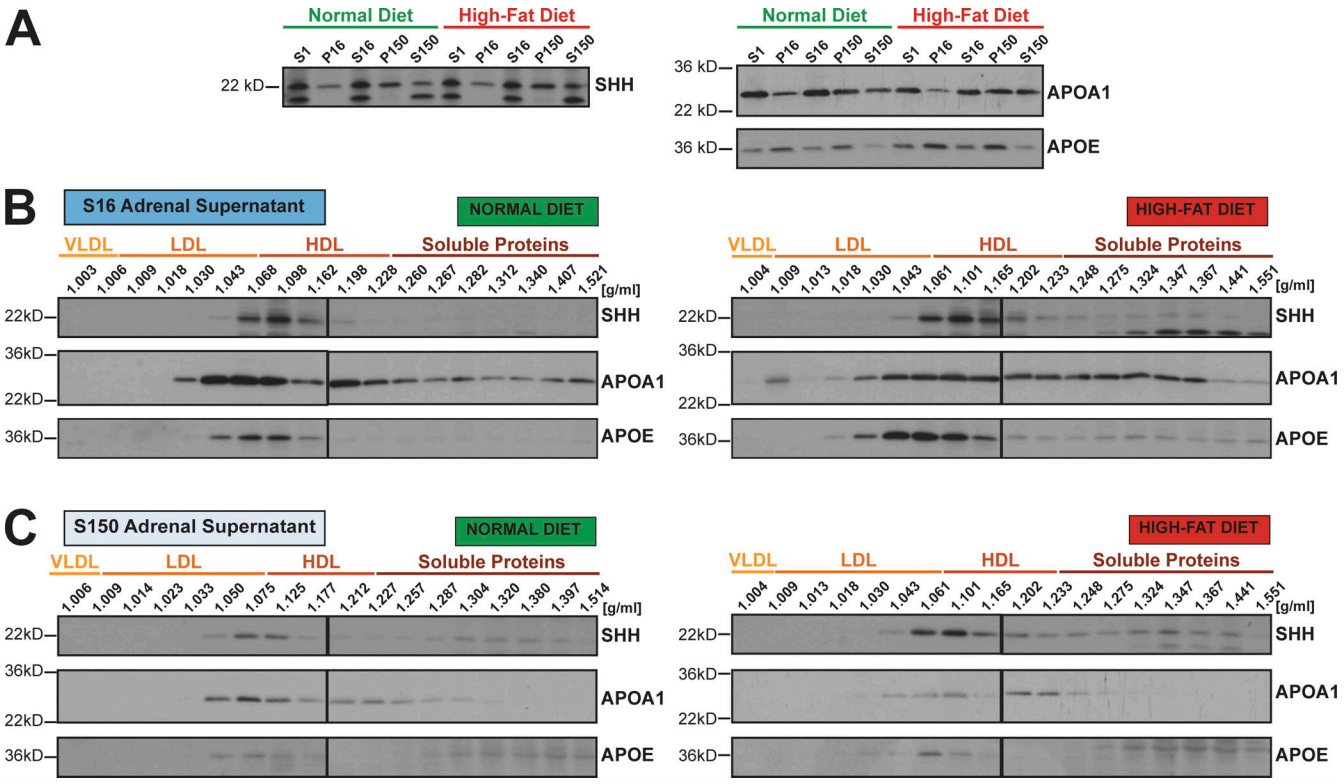

Figure S1. **HFD-induced obesity does not change the fractionation of SHH or lipoproteins in the adrenal gland. (A)** Western blots of lysed adrenals isolated from mice fed a normal diet or a HFD, fractionated by differential centrifugation, probed for SHH and lipoprotein markers. **(B)** Western blots of density gradient fractions from adrenal supernatants at 16,000 *g* and 150,000 *g* of mice fed a normal diet or a HFD, probed for SHH and lipoprotein markers. Density of lipoprotein classes is according to Jonas and Phillips (2008). The experiment was repeated two times with similar results. VLDL, very-low-density lipoproteins.

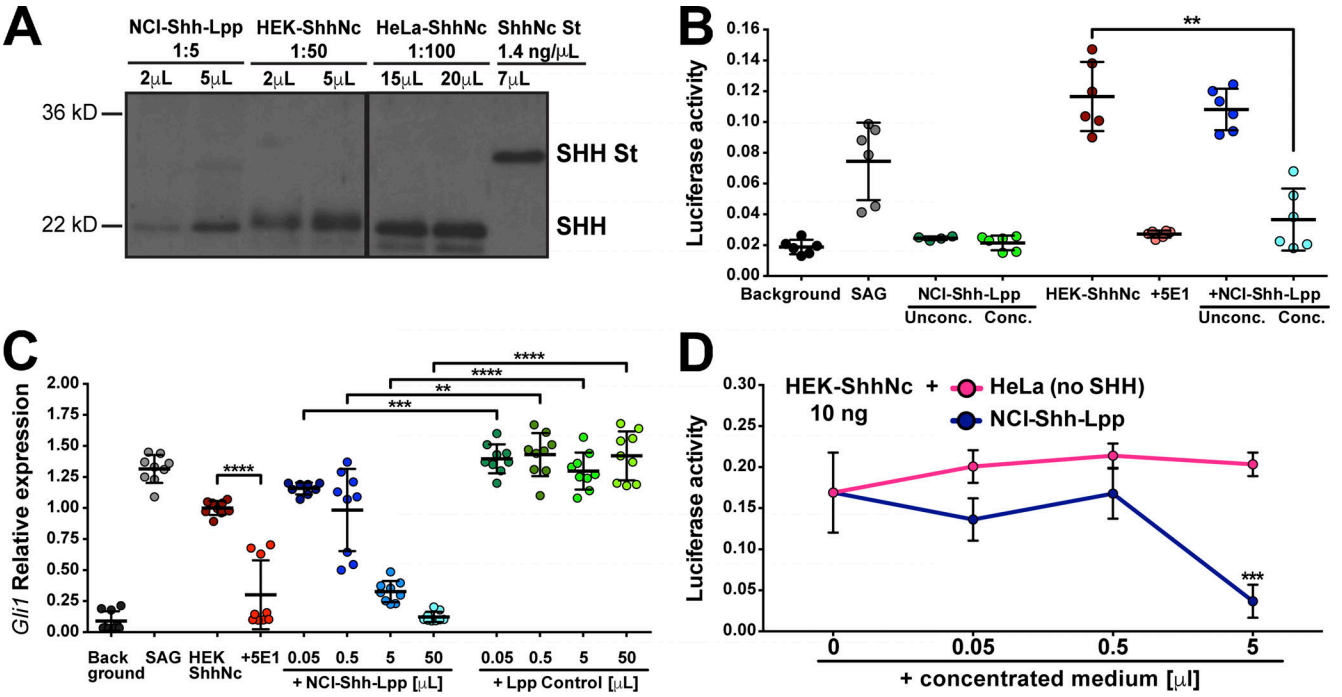

Figure S2. **NCI-H295R–derived conditioned medium inhibits SHH signaling activity. (A)** NCI-H295R cells secrete lower amount of endogenously produced SHH than SHH-transfected HEK-293 and HeLa cells. Western blot of SHH-containing conditioned media from NCI-H295R (NCI-Shh-Lpp), HEK-293 (HEK-ShhNc), and HeLa cells (HeLa-ShhNc). Loading volumes and dilutions of the media were adjusted so that all samples have similar blotting intensity. SHH St is control SHH protein, engineered from mouse Shh sequence with an N terminus His tag, enterokinase cleavage sequence (DDDDK), and 2× Ile replacing the first Met (molecular weight = 24.5 kD). The amount of secreted NCI-Shh-Lpp is ∼10× lower than HEK-ShhNc and 60× lower than HeLa-ShhNc. **(B)** Shh-LIGHT2 cells were treated with the same amount of concentrated or unconcentrated NCI-H295R–conditioned medium, alone or together with HEK-ShhNc. Treatment with the SMO-agonist SAG is a positive control for Shh-LIGHT2 assay activity. Treatment with anti-SHH 5E1 antibody together with HEK-ShhNc is a positive control for the inhibition of HEK-ShhNc signaling activity. **(C)** *Gli1* expression in Shh-LIGHT2 cells treated with 200 nM SAG, 10 ng HEK-ShhNc alone or together with 10 µg/ml 5E1 or increasing amounts of NCI-H295R–conditioned medium (NCI-Shh-Lpp) or the appropriate medium control (Lpp Control). *B-actin* was used as a reference. Data are normalized to the values for relative *Gli1* expression in HEK-ShhNc–treated cells. **(D)** Shh-LIGHT2 cells were treated with 10 ng HEK-ShhNc together with increasing amounts of 100× concentrated HeLa (not transfected with SHH) or NCI-H295R–conditioned medium. **(B–D)** Data are presented as mean ± SD, *n* = 6–9 replicates, pooled from three experiments. **, P < 0.01; ***, P < 0.001; **** P < 0.0001.

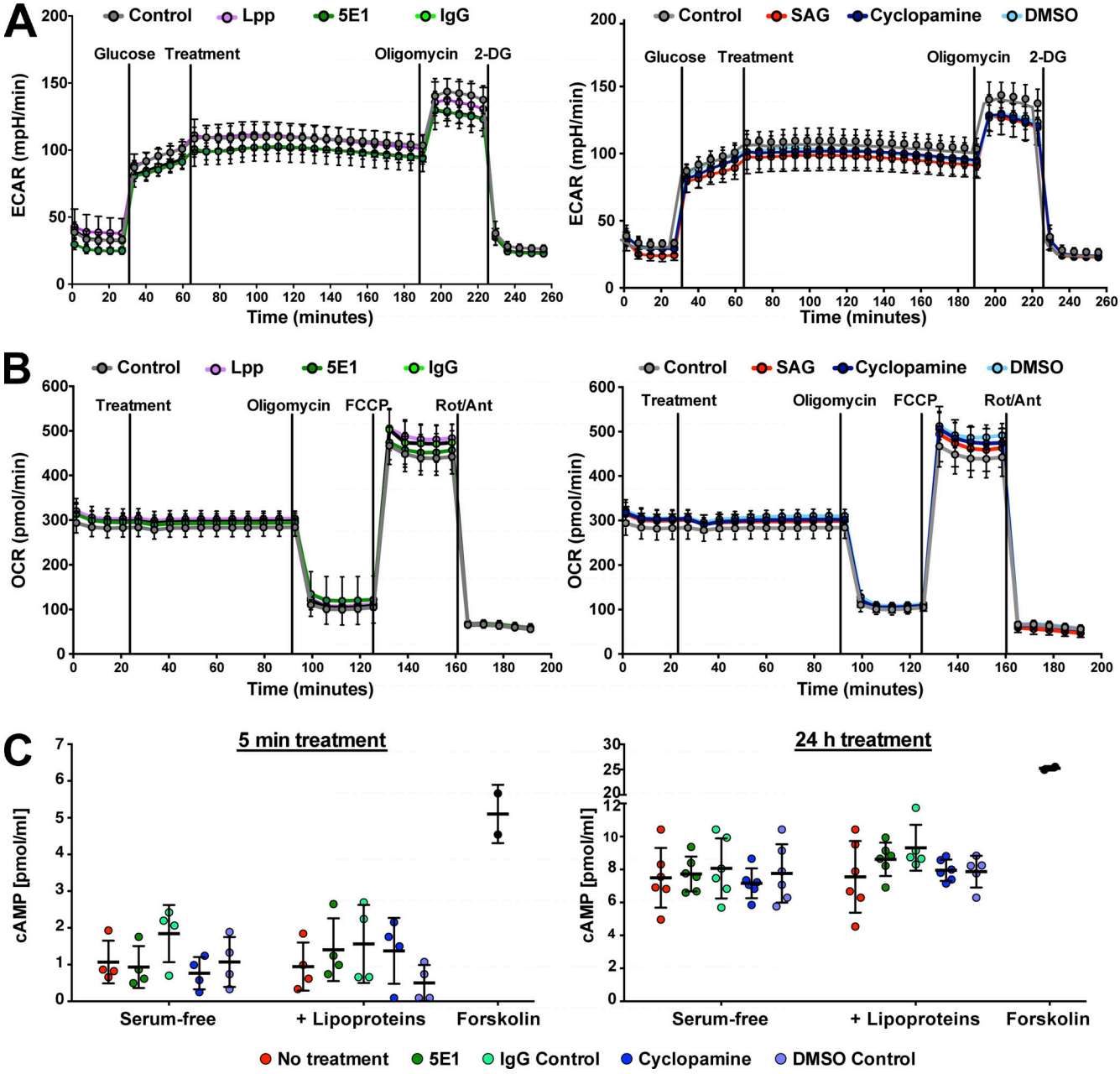

Figure S3. **Human adrenocortical carcinoma cells do not respond to autocrine noncanonical SHH signaling. (A and B)** Measurement of extracellular acidification rate (ECAR; A) and oxygen consumption rate (OCR; B) with Seahorse technology after treatment of NCI-H295R cells grown in serum-free conditions with the SHH pathway inhibitors, 10 µg/ml 5E1 or 10 µM cyclopamine or 200 nM SAG and appropriate controls. *n* = 12 replicates from two independent experiments, presented as mean ± SD. **(C and D)** Measurement of intracellular cAMP levels in NCI-H295R cells, cultured in serum-free medium or with the respective treatments (10 µg/ml 5E1, 10 µM cyclopamine, 200 nM SAG and appropriate controls) after 5 min (C) or 24 h (D). Treatment with 20 µM forskolin was used as a positive control for induction of cAMP production in NCI-H295R cells. Data are presented as mean ± SD, *n* = 6 replicates, pooled from three experiments. 2-DG, 2-deoxy-D-glucose; FCCP, carbonyl cyanide 4-(trifluoromethoxy)phenylhydrazone; LPP, humapn lipoproteins; mpH, milli pH; Rot/Ant, Rotenone/Antimycin A.

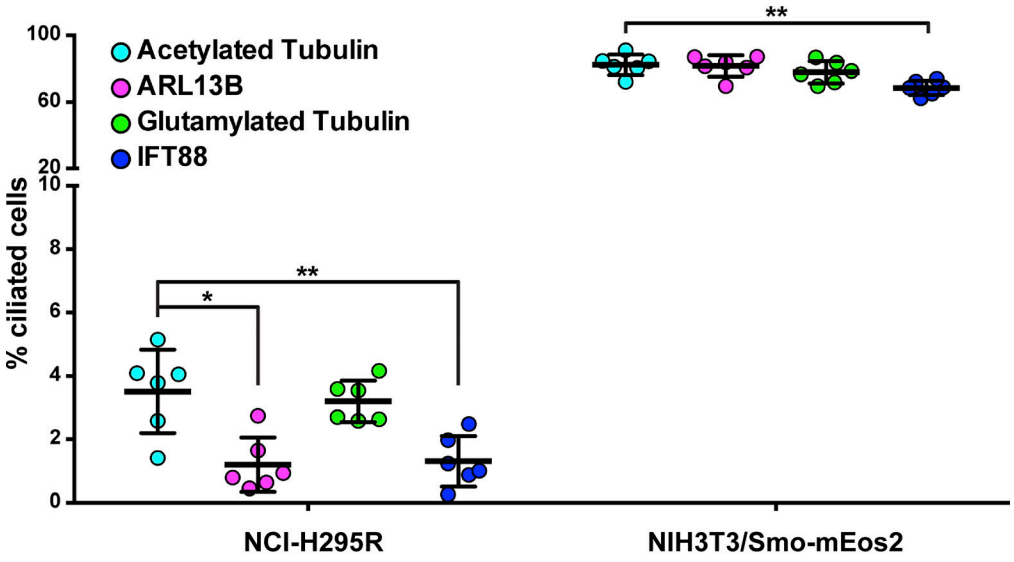

AcTUB	2597	1728
ARL13B	2377	2093
GlutTUB	3004	2060
IFT88	1970	1761

Figure S4. **NCI-H295R cells are poorly ciliated.** Quantification of the percentage of ciliated NCI-H295R and NIH3T3/Smo-mEos2 cells, counted as cells positive for each of the ciliary markers: acetylated tubulin (AcTUB), ARL13B, glutamylated tubulin (GlutTUB), or IFT88. The number of counted cells is given under the graph. Data are presented as mean ± SD, *n* = 6 replicates, pooled from three experiments. *, P < 0.05; **, P < 0.01.

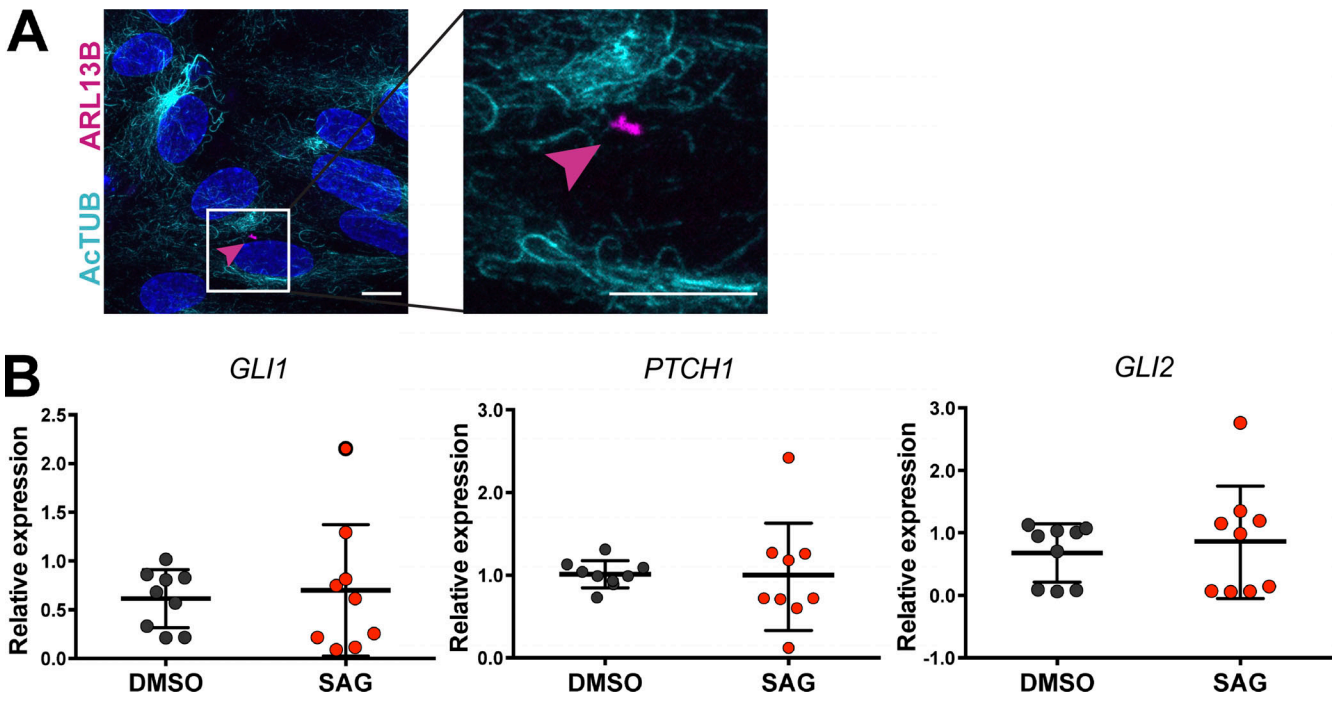

Figure S5. **HUVECs do not respond to canonical SHH signaling. (A)** Immunofluorescence of HUVECs stained for acetylated tubulin (AcTUB; cyan), ARL13B (magenta), and nuclear DAPI (blue). Magenta arrowhead denotes an ARL13B-positive cilium. From 419 cells counted, 0.95% were positive for ARL13B. Scale bar, 10 µm. *n* = 3 replicates. **(B)** Quantitative RT-PCR for *GLI1*, *PTCH1*, and *GLI2* expression in HUVECs treated with SAG (200 nM) for 24 h, using *18S* rRNA as an internal control. Data are presented as mean ± SD, *n* = 9 replicates, pooled from three experiments.